

FACULDADE DE ENGENHARIA DA UNIVERSIDADE DO PORTO



FEUP FACULDADE DE ENGENHARIA
UNIVERSIDADE DO PORTO

Modeling and Performance Evaluation of Bicycle-to-X Communication Networks

José Bastos Pintor

WORKING VERSION

Mestrado Integrado em Engenharia Eletrotécnica e de Computadores

Supervisor: Pedro Miguel Salgueiro dos Santos

Second Supervisor: Pedro Miranda de Andrade de Albuquerque d'Orey

February 22, 2019

© José Bastos Pintor, 2018

Resumo

Com o crescimento da conectividade dos veículos e utilizadores vulneráveis de estrada, como pedestres e ciclistas, permite a exploração de soluções para a segurança e aplicações de partilha de informação com base nas tecnologias de comunicação wireless. O comportamento destas tecnologias é afectado pelo meio que penetra, como em carros, bicicletas e pessoas, mas algumas destas tecnologias conseguem penetrar nestes meios de forma similar entre eles. Wifi é uma destas tecnologias e que está actualmente presente nos smartphones e no interior de alguns carros como hotspots. Esta tese tem como objectivo caracterizar experimentalmente a performance desta ligação sem fios e desenvolver um modelo para estimar a potencia de sinal recebida (RSSI) entre dispositivos WiFi instalados em bicicletas e em carros equipados com APs WiFi embutidos.

O modelo de estimação de RSSI extende modelos empíricos já existentes (como o modelo de Log-Distance Path Loss e Two-Rays Ground Reflection Path Loss), incluindo a obstrução causada pelo conjunto da bicileta e o ciclista e de um veículo também. Nós também avaliamos a pertinencia do uso do hotspot do carro para aplicações de segurança/informação.

Nós começamos por caracterizar o padrão de radiação a partir de varios pontos onde a antena foi instalada na bicicleta, para reduzir o número de posições para montar a antena nas medições que se seguirem.

Depois, nós medimos o padrão de radiação do sistema bicicleta-ciclista e o padrão de radiação de um carro com WiFi embutido e de um AP WiFi instalado por nós.

No final, nós avaliamos o desempenho do modelo comparando a estimativa do RSSI e as amostras capturadas em cenários de interação bicicleta-carro: (i) o ciclista ultrapassa um carro estacionado, (ii) um cruzamento com linha de vista (LOS).

Observamos que: no cenário (i), 65% das estimativas de RSSI, o nosso modelo estima dentro de um intervalo de ± 5 dBs; para (ii), cerca de 45% do valores amostrados estão entre ± 5 dBs da previsão, enquanto o modelo subestima cerca de 27% dos valores entre -5 dBs e -10 dBs.

Os nossos resultados empíricos também demonstraram que é possível usar de forma oportuna um sistema de comunicação ad-hoc para varios tipos de aplicações, especialmente nos cenários de mais relevancia como a aproximação do ciclista ao carro (i.e., o IRT é menor que 400 ms e o throughput é à volta de 3 MBytes), e que o corpo humano, a estrutura do veículo e o tipo de cenário influenciam a qualidade da ligação e a performance do sistema em termos de IRT.

Abstract

The growing connectivity of vehicles and Vulnerable Road Users, i.e., pedestrians and cyclists, allows to explore solutions based on wireless communication to support safety, efficiency and infotainment applications. However, there are few communication technologies that enjoy similar penetration ratios on cars, bicycles and pedestrians. WiFi is one of such technologies, as can be found in smart phones and in on-board hotspots. This thesis aims to characterize experimentally the wireless link performance and develop a model to estimate the received signal strength (RSSI) between WiFi devices installed on bicycles and cars equipped with built-in WiFi APs. We have also evaluated the pertinence of the car's hotspot for safety/infotainment applications.

The RSSI estimation model extends existing empirical models (e.g., the Log-Distance Path Loss model) by including the shadowing of the bicycle-and-cyclist system and of a vehicle. We first characterize the radiation pattern of antennas installed in several mounting points of a bicycle, in order to reduce the set of mounting points to be explored in future measurements. We then measured the radiation pattern of the bicycle and cyclist system, and the radiation pattern of a car with built-in and dedicated WiFi access points. Finally, we evaluate the performance of the model by comparing RSSI estimates and measurements collected in selected interaction scenarios between bicycles and car: (i) bicycle overtaking a parked car, (ii) perpendicular crossing with LoS. We observed that: for (i), 65% of the RSSI estimates our model estimates within the range of ± 5 dBs; for (ii), about 45% of the measured values of RSSI are between ± 5 dBs the prediction, while it underestimates about 27% of measured values within -5 dBs and -10 dBs. Concerning link performance, our empirical results have also shown that an opportunistic ad-hoc communication system is able to support a variety of applications, specially in the most relevant scenario where the bicycle approaches a car (i.e., the IRT is below 400 ms and the throughput is around 3 MBytes), and that human, vehicle structure shadowing and the scenario type affect the link quality and the system performance in terms of IRT.

Acknowledgements

I would like to thank:

- IT-Porto for their financial support and taking me in their offices and project;
- The GenerationMobi. team for their support.
- Pedro Santos and Pedro D’Orey for their constant support and guidance, for their input and patience, and for always being present.
- Hugo Santos from INESC-TEC for providing help setting up and providing support for the experiments that required the anechoic chamber.
- My friends and colleagues that have been there from the start of this academic journey, namely: Ana Cunha, André Morais, Bruno Conceição, Diogo Martins, Filipa Nunes, João Polónia, José Pedro Gomes, Pedro Ferreira, Sara Lemos, Tiago Fonseca, Tiago Dias and Vitor Fernandes.
- I would like to also thank my karaté team Clube Karaté da Maia, and my master Jorge Sousa for providing a punching bag to discharge all the stress from studying.
- I want to thank professor Lucinda Ralha which had a great influence in all of my academic career.
- Lastly but certainly not least, my very best friend Ana Cruz for putting up with me everyday and my family for all the love, care and support they constantly deliver on a daily basis like no one does.

José Pintor

“Anything that can go wrong will go wrong”

Edward A. Murphy

Contents

1	Introduction	1
1.1	Context and motivation	1
1.2	Objectives and Contributions	2
1.3	Scope and Structure of the Document	3
2	Related Work	5
2.1	Applications of VRU-to-X Communications	5
2.2	Characterization of Vehicular Links and Propagation	7
2.2.1	Link Characterization	7
2.2.2	Propagation Models and RSSI Estimation	8
2.2.3	Antenna Positioning and Vehicle-Induced Shadowing	10
2.3	Discussion and Conclusion	11
3	Experimental Characterization of 802.11 Vehicular Radiation and Path Loss	13
3.1	Common Experimental Setup	14
3.2	Study on antenna positioning on bicycles	14
3.2.1	Experimental methodology	15
3.2.2	Results	17
3.2.3	Discussion on Quality of Antenna Positions and Final Remarks	20
3.3	Bicycle-cyclist Shadowing	20
3.3.1	Experimental methodology	21
3.3.2	Results	22
3.3.3	Remarks and Discussion on Antenna Positioning	24
3.4	Car Shadowing	24
3.4.1	Experimental methodology	25
3.4.2	Results	26
3.4.3	Conclusion and discussion	28
3.5	Path Loss Evaluation	29
3.6	Experiments Conclusion	30
4	Evaluation of B2X Propagation Model	31
4.1	The B2C model	31
4.2	Validation Scenarios	32
4.3	Experimental methodology	33
4.4	Results	34
4.4.1	Parallel scenario	35
4.4.2	Perpendicular scenario	39
4.5	Conclusion	42

5 Opportunistic Use of In-Vehicle Wireless Networks for VRU Interaction	43
5.1 Experimental Evaluation and Results	43
5.2 Conclusion	46
6 Conclusion	47
6.1 Final thoughts	47
6.2 Future work	48
A Appendix	49
A.1 The B2C model in a non LoS scenario	49
A.1.1 Results in a non LoS scenario	49

List of Figures

3.1	(a) Selected antenna positions for the link characterization, namely 1) handlebar, 2) under seat, 3) back rack, 4) back wheel, 5) chain side of back wheel, 6) inner frame, 7) front wheel and (b) Depiction of anechoic chamber setup with rotating platform under the bicycle	15
3.2	Antennas setup	17
3.3	Antenna's RSSI pattern over different mounted positions on the bicycle, which is facing to 0 degrees	18
3.4	Experimental setup used for human shadowing experiment. (a) The bicycle is centered to 4 tripods in a 5 meters radius with antennas mounted. After a capturing session, the bicycle will rotate 22,5 degrees, which will have a new angle perspective from each. At the end of 4 rotations the samples will have 16 angles captured with a step of 22,5.	22
3.5	Antenna's RSSI pattern over different mounted positions on the bicycle, which is facing to 0 degrees, with and without a rider: (a) middle point of handle bar (b) left grip of handle bar (c) bicycle's back rack	23
3.6	(a) Experiment location and (b) antenna setup in car	25
3.7	(a) Depiction of vertical angle interference in communication and of (b) car radiation pattern captured angles from experimentation	26
3.8	Normalized average RSSI (left) and standard deviation (right) of measured RSSI for the DME and PE setups installed in the car, and different TX-RX separations. The vehicle's front is aligned with the angle 0	27
3.9	(a) Side-view of the test car including location of the in-vehicle antennas for the dedicated measurement equipment (1) and production equipment (2) setups (b) The production equipment antennas is located under the shark fin of the car.	28
3.10	Measured data, and fitted log-distance and two-ray ground models.	29
4.1	Selected representative scenarios: (a) parallel movement of bicycle overtaking parked car; (b) perpendicular movement in crossing roads with LoS;	32
4.2	Experimental setup used in DME and PE setup with GPS tracker and antennas on the car's rear-view mirror	34
4.3	RSSI Samples (green dots) from the parallel scene , overlaid with RSSI model prediction using either (a) Log Distance model or (b) Two-Rays model as the path loss component and comparison of the introduction of influence of bicycle-cyclist and car's bodies (red line) to their absence (blue line).	36
4.4	RSSI attenuation contributed by cyclist-bike (blue) and car (red) bodies in the B2C model for the parallel scenario	37

4.5	Histograms for performance of the B2C model for the parallel scene , using (a) Log Distance, (b) Two-Ray Ground Reflection as path models, and (c) comparing each other's performances	38
4.6	RSSI Samples (green dots) from the perpendicular scene , overlaid with RSSI model prediction using either (a) Log Distance (B2C is orange, LD is blue) , (b) Two-Ray Ground Reflection as path models (B2C is orange, TR is blue), and (c) comparing each other's performances (TR is orange, LD is blue).	39
4.7	RSSI attenuation contributed by cyclist-bike (blue) and car (red) bodies in the B2C model for the perpendicular scenario	40
4.8	Histograms for performance of the B2C model for the perpendicular scene , using (a) Log Distance (B2C is orange, LD is blue) , (b) Two-Ray Ground Reflection as path models (B2C is orange, TR is blue), and (c) comparing each other's performances (TR is orange, LD is blue)	41
5.1	Received Signal Strength Indicator (RSSI) Empirical Distribution Function for two scenarios using PE and DME.	44
5.2	Received Signal Strength Indicator (RSSI). For each 10 m distance bin, we represent the mean RSSI and the corresponding one standard deviation around the mean.	45
5.3	Throughput as a function of distance for DME. Each point corresponds to the average throughput per 1 s interval.	45
5.4	Packet Inter-reception Time (IRT) CDF for Parallel and Perpendicular scenarios using Production Equipment (PE).	46
A.1	Depiction of NLoS scenario	50
A.2	Location and bike's path used to capture RSSI samples for a scenario with no Line-of-Sight. Figure (c) depicts the road to the right of the car, and (d) to the left side.	51
A.3	RSSI Samples (green dots) from the perpendicular scene without LoS , overlaid with RSSI model prediction using either (a) Log Distance model or (b) Two-Rays model as the path loss component and comparison of the introduction of influence of bicycle-cyclist and car's bodies (red line) to their absence (blue line).	52
A.4	Histograms of errors of the model for the perpendicular scene with LoS, using Log Distance, Two-Rays as path models, (a) comparing its performances between each other and their free space counterparts: (b) LD (c) TR	53

List of Tables

2.1	Resume table of applications	7
3.1	Configured parameters for the wifi antennas	14
3.2	Statistical values from results data	19

Acronyms and Symbols

AP	Access Point
ACL	Asynchronous Connection-Less Link
B2C	Bicycle to car
B2V	Bicycle to vehicle
Bi2Bi	Bicycle to Bicycle
BPSK	Binary Phase-Shift Keying
C2B	Car to bicycle
CACC	Cooperative Adaptive Cruise Control
CDF	Cumulative Distribution Function
DME	Dedicated Measurement Equipment
DSRC	Dedicated Short Range Communications
ERTM	Enhanced Retransmission Mode
FEC	Forward Error Correction
GEMV2V	the Geometry-based Efficient propagation Model for V2V
GPS	Global Position System
IEEE	Institute of Electrical and Electronics Engineers
IRT	Inter-reception Time
ITS	Intelligent Transport Systems
LD	Log-distance path loss model
LoS	Line Of Sight
M2M	Machine to Machine
NLoS	Non Line of Sight
PE	Production Equipment
PER	Packet Error Rate
QAM	Quadrature Amplitude Modulation
QPSK	Quadrature Phase-Shift Keying
QoS	Quality of Service
RSSI	Received Signal Strength Indicator
RLR	Red Light Runners
SVM	Support Vector Machine
TCP	Transport Control Protocol
TR	Two-Ray Ground Reflection path loss model
USB	Universal Serial Bus
UDP	User Datagram Protocol
WAVE	Wireless Access in Vehicular Environments
VANET	Vehicular Ad-hoc Networks
V2V	Vehicular to Vehicular
V2X	Vehicular to any
VRU	Vulnerable Road Users

Chapter 1

Introduction

This chapter presents the context and motivation of this thesis in Section 1.1, the goals and expected contributions to the problem at hand in Section 1.2, and the structure of the document in Section 1.3.

1.1 Context and motivation

Nowadays, people rely increasingly more on Internet access for connecting to other people and accessing online services. This tendency extends to machines and there is a growing trend to explore direct communication between people, between people and machines, and machine to machine communications (M2M). One notable example is the communication between vehicles (e.g., cars, bicycles) that enables a number of safety, efficiency and infotainment applications. This thesis focus specifically on communication between bicycles and other road-using parties.

Cycling is not only a great benefit for the health of every person, it also improves the traffic flow in cities[1]. In 2016, roughly 12% of the population in USA used a bike in their everyday life as a mean of transportation [2]. Cyclists and the pedestrians are considered Vulnerable Road Users (VRUs) given to their lower levels of protection in case of road accidents. In 2015, 818 cyclists died in crashes with motor vehicles and over 45,000 cyclists were involved in accidents in USA [3]. Accidents have a profound social and economic impact.

Many of such accidents are caused by driver inattention, lack of situation awareness or misunderstanding the intentions of other road users. If cyclists and the drivers could be aware earlier the presence of one another, these alarming statistics could be certainly greatly decreased. Increasing the awareness of road users could be achieved through the use of wireless communications, namely by the broadcast of frequent beaconing packets (*here I am*). The introduction of batteries in bicycles facilitates the installation of communication devices in these energy-constrained vehicles. This communication system will enable a number of applications, namely safety (e.g. crossing vehicles [4]), efficiency (e.g. bicycle platooning [5]) and infotainment (e.g. audio and visual communication [6]). However, few works evaluate communication technologies between bicycles and cars, and analyze their perform in several distinguishing scenarios.

While the existing standard for vehicular communications (802.11p) has yet to reach widespread adoption, the DSRC equipment and products has not yet reached large-scale production and a diversified product offer. Thus, there are few products offering DSRC communication with a form factor adequate for bicycles. On the other hand, the abundance of devices with WiFi is greatly vast nowadays, from phones to cars with APs, creating a creative space for the development of vehicular applications that can promote more safety for drivers and VRUs. An application designer wishing to develop vehicular applications based on wireless bicycle-to-X communication needs to have a characterization of the quality of the link, in terms of e.g. throughput, PDR, received signal strength (RSSI), to manage its limitations and draw expectations about the communication behavior. Many factors could influence the quality of a link when operating in an high frequency band, such as obstruction from other vehicles [7] and/or objects (e.g. trees, traffic lights), interference from other devices operating in the same frequency band [8] and the considerable impact of the user and the vehicle's geometry.

1.2 Objectives and Contributions

The bicycle-to-vehicle (B2V) communication link presents the following distinguishing features that have not been considered *jointly* in previous V2X studies, namely: (1) the signal degradation due to antenna location on a bicycle, (2) the presence of additional objects and infrastructures specific to this scenario (e.g. human body, bicycle frame, in-car objects) leading to fewer Line-of-Sight (LoS) opportunities, (3) mobility of both communication nodes (e.g. as opposed to communication to static 802.11 hotspots) that impairs differently the signal propagation.

Thus, the goal of this dissertation is two-fold:

- Characterize the B2V physical channel in terms of the Received Signal Strength (RSS) and propose a propagation model for that scenario, the B2C model;
- Characterize the B2V communication in terms of data link metrics (throughput, IRT).

The performance analyses of the WiFi technology in terms of physical layer metrics and data link will allow to make better decisions at the time of designing an application that relies on the capacity of communication at various distances, how far to maintain a connection and the quality of the link. We now describe each of these goals in additional detail.

The B2C Propagation Model: building on the existing numerous models for vehicular communications [9], we propose to include the contribution of the shadowing caused by the cyclist-bicycle system and car structure and elements. We use a path loss model and add our contribution of shadowing caused by vehicles frames, the new elements L_B and L_C , respectively, as shown in Eq. 1.1. This modular approach leaves open the possibility of improving each element individually and independently of the others.

$$P_{RX} = P_{TX} + L_{path_loss}(d) + L_B(\gamma) + L_C(\gamma) + X_\sigma \quad (1.1)$$

The elements of the B2C model must be obtained empirically through a large-scale measurement campaign. Thus we have carried a number of experiments to feed our model and evaluate its performance.

Link Characterization: where there is LoS, we also assess V2B link quality using three conventional metrics, namely RSSI, Throughput and Packet Inter-reception Time (IRT), where the two later metrics inform about the Quality of Service (QoS) offered to VRU protection or interaction applications. Coincidentally, we have compared the performance of a car's hotspot product equipment with our own dedicated measurement equipment and evaluate its pertinence in a vehicular network.

The main contributions of this thesis are:

- characterization of radiation of an antenna in selected installation positions in a bicycle (in anechoic chamber), so we can assess the impact of the metal structure of the bicycle in the link;
- radiation patterns of a bicycle equipped with an antenna and with a cyclist, and of a vehicle, both for the in-car WiFi AP and for a dedicated wireless module;
- a model that computes RSSI estimates between vehicular nodes, specifically bicycles and/or cars, and that is evaluated against real-world measurements;
- assess the performance of two WiFi systems performing for two representative scenarios with LoS to various metrics, so we can study its reliability;
- opportunistic usage of a car's AP as a stepping stone for the development of safety and infotainment applications.

1.3 Scope and Structure of the Document

The remainder structure of this thesis is as follows. In Chapter 2 we review the state of the art and compare all the related work to this thesis. The experimental procedures to obtain empirical models for each element of the propagation model are described in Chapter 3. Chapter 4 further details the B2C model and presents how we validate it. In Chapter 5 we present the measurements with the usage of the car's built-in WiFi device and compare them to our own setup. The conclusion and future work is presented in Chapter 6.

Chapter 2

Related Work

In this chapter, the relevant state of the art is described. Two broad topics are relevant for this thesis, namely applications of bicycle-to-X communications, and characterization of vehicular links and networking. Section 2.1 presents several applications that can be developed on top of wireless communication systems and how they rely on their performance. Section 2.2 characterizes selected wireless communication technologies and how these technologies can support these applications on vehicular networks. Since there are only a few relevant studies regarding these technologies with bicycles, works done on scooters and other vehicles applying these technologies are also taken to consideration in this review.

2.1 Applications of VRU-to-X Communications

There are a number of works that propose applications over vehicular links for safety, efficiency and infotainment applications. We identify relevant applications and their requirements, that the underlying communication system must provide. Applications are designed to its developer will and could go from smartphones from the drivers that exchange data with other smartphones from other drivers or VRUs, to on-board/built-in devices that interact with another vehicle with them installed. Most of them work as safety measures and alert the user of the presence of another VRU.

Kuang-Shih Huang et al. [10] describes a scooter avoidance system that can identify red-light runners (RLRs) at intersections. The solution is infrastructure-free and relies on ad hoc communication between the passengers' smartphones that are equipped with IEEE 802.11b/g/n WiFi radio. The smartphone on board predicts if the scooter driver will reach the intersection before the red light or not; and if it is predicted that it will run the red light, the system tells the driver to decelerate immediately. The prediction is based on a classifier: an SVM algorithm that learns the RLR behavior. In realistic field experiments, they have concluded that their proposed system can help prevent 70% of collisions that violate the traffic signals, with a false alarm at 5%.

José Santa, Pedro Fernández, and Miguel Zamor [6] have integrated two-wheeled vehicles in a vehicular network by designing a wireless communication device for cyclists and motorcyclists. The embedded communication node for two-wheeled includes proper software to warn the driver

of approaching of other vehicles through audio and visual notifications. These warning messages are exchanged through IEEE 802.11 p communications between vehicles, while IEEE 802.11 b/g is used to communicate with smartphones. An android app is yet to be developed and run performance tests, although their initial validation tests were positive.

Sandra Céspedes et al.[5], the authors propose a system that coordinates individuals in a cycling group while maintaining each individual goal. They employ a Cooperative Adaptive Cruise Control (CACC), a speed recommendation system for the cyclist. Upon reception of information, the smart bicycles recalculate its acceleration and adjusts the program of action to be adopted by its cyclist to adjust to the rest of the platoon. They have run simulations with four nodes, each using IEEE 802.15.4 interfaces and concluded that the CACC improved individual goals to be achieved and that cyclists can effectively respond to haptic signals.

B. Kihei, J. A. Copeland, and Y. Chang[4], the authors present a system that provides collision avoidance using Received Signal Strength Indication (RSSI) in V2V networks. This system requires that the vehicles are equipped with a DSRC radio that can listen to the WAVE-802.11p standard. They have then conducted three scenarios with two cars equipped with such radios, centered on the roof. These scenarios are: i) Cross path with no line-of-sight; ii) Same lane, approaching rear-end and iii) Moving in opposite directions. The authors have concluded that this system needs enhancements to reduce the false alarm rate and increase the detection rate for large variances in serious channel conditions. Nevertheless, this system has predicted 35% more collision than the traditional RSS-distance method.

K. Dhondge et al. [11], the authors propose a smartphone based Car-to-X communication system that alerts the driver of possible collisions to VRUs and another vehicles that they have named "WifiHonk". They try to predict the collision by: when another vehicle is detected (through sensing RSSI of WiFi beacons of smart devices), the driver's phone computes how much time it has to stop and when it should stop, and draws conclusions from there. In their work they try to correlate the RSSI value of a beacon that is received on the other end to the distance between the two devices. From their practical and simulation experiments, they say that WifiHonk works well up to 113 km/h for high speed vehicles and successfully exchange warnings between VRUs and vehicles.

R. Parker and S. Valae [12] show a cooperative-vehicle-position-estimation algorithm they have developed to compete with GPS-based current solutions. They have run simulations that make measurements of distances between vehicles using IEEE 802.11p through a radio-ranging technique. This technique is a algorithm that uses signal-strength-based inter-vehicle distance measurements, vehicles kinematics, and road maps to estimate the relative positions of vehicles in a cluster. In the end, they have concluded that the RSSI solutions can be more accurate than the actual GPS-based position solutions and improved by taking into account extra information, such as maps of the road, vehicle kinematics, etc.

S. Hisaka and S. Kamijo [13], the authors developed a on-board ‘sensor’ utilizing wireless communication devices for collision avoidance around corner intersections. This ‘sensor’ consists of four wireless IEEE 802.15.4 receivers. The position direction, distances and motions of other

Aspect	Studied technology	Used vehicle	Scenarios
Red-Light Runners[10]	WiFi	Scooter	Crossing
ITS for two-wheelers[6]	WiFi and IEEE 802.11p	Two-wheeled	Not clear
Platoon Cooperation[5]	IEEE 802.15.4	Smart bicycles	Platoon
Predicting Car Collision[4]	IEEE 802.11p	Cars	Crossing and parallel
WiFi Honk[11]	WiFi	Cars	Crossing and parallel
Vehicular Localization[12]	IEEE 802.11p	Cars	Any
RSSI Sensors[13]	IEEE 802.15.4	Cars	Crossing

Table 2.1: Resume table of applications

vehicles can be detected by comparing four sequences of RSSI of receivers. After testing they have successfully detected pedestrians walking near the driver's vehicle turning and detect vehicles that are approaching the intersection from far (nearly 30m).

Table 2.1 resumes these communications based on the used technology, the vehicles they were tested with and in the scenario they were tested or designed for.

2.2 Characterization of Vehicular Links and Propagation

We review previous work on vehicular networks that include bicycles and other vehicles, that show how these networks are integrated and evaluate the communications limits.

This section is divided into three subsections in which we: observe others works on characterizing links with wireless technologies; we describe studied of propagation models in the free space; others works related to signal degradation through shadowing.

2.2.1 Link Characterization

The following works focus on characterizing links of wireless technologies which methodologies are relevant because of the vehicles used and the conclusions they drawn from their experimentation.

Hao-Min Lin, Hsin-Mu Tsai, and Mate Boban [14] characterize the communication performance between a scooter and another vehicle with short-range communications utilizing IEEE 802.15.4 radios (Zigbee). The authors assess the additional signal attenuation caused by the driver and the passenger of the scooter and propose a model that takes into account the attenuation due to body-shadowing. They concluded that the best position for the antenna on a scooter would be on top of the scooters side mirror because it's the furthest from the frame and the highest possible point to mount the antenna in the scooter. They have also concluded that the additional signal attenuation by body shadowing of the driver and passenger was on average a range from 9 to 18 dB.

Richard Gass, James Scott, and Christophe Diot [15], the authors measured the performance of UDP and TCP wireless transfers between a mobile device in a moving car and a 802.11b access point. They focus on the impact of bandwidth and delay limitations in the backhaul network and on

the feasibility of in-motion transfer with typical internet applications. In conclusion, they found out that the application's performance suffers mostly from the network or application's issues (i.e. protocols which have hand-shakes, bandwidth limitations, long round-trip times) and that the 802.11 technology still provides a reliable data transfer and high throughput, even for small effective communication windows: (1) the client could see beacons from 412 meters to 330 meters at 5 to 75mph, but only associate correctly when 272 to 143m away from the AP; (2) the effective window does not vary much but the time spent in that window does dramatically, from 217 second at 5mph to only 13.7 seconds at 75 mph.

A. P. Subramanian et al. [16], the authors present a directional antenna mounted on a moving vehicle that localizes roadside WiFi access points (APs) located outside or inside of buildings. They highlight how they estimate the angle of arrival of frames transmitted from the AP using RSSI on different directional beams of the antenna. Their main contributions are: identifying that signal reflections can cause significant localization errors and developing a clustering method to solve this problem. This system has shown to be very accurate when it comes to locate the client using WiFi 802.11b/g, with a margin errors between 10-30 meters in the toughest scenarios (inside buildings).

2.2.2 Propagation Models and RSSI Estimation

The Friis Transmission formula is the basis for the free-space path loss model, i.e., with out obstructions [9]. In a condensed version in the logarithmic domain, it identifies the power gains and attenuation in a transmission link :

$$P_{RX} = P_{TX} + G_{TX} + G_{RX} + L_{free_space} \quad (2.1)$$

Where P is power, either measured or emitted, and G is the Gain from the emitter (TX), receiver (RX) and free space.

In real-world scenarios with complex propagation, when field measurements are available, an empirical channel model can be estimated. The equation 2.2 is such an empirical model for wireless channels: the Log-Distance Path Loss Model [9].

$$P_{RX} = P_0 + 10 * \log\left(\frac{d}{d_0}\right) * \alpha \quad (2.2)$$

Where P_{RX} is the received power of a signal through a path with attenuation of α dB/meters at a distance d, P_0 is the reference power, and $10 * \log(d/d_0) * \alpha$ is the power lost through path loss.

The Two-Ray Ground Reflected Model [17] predicts path losses between two nodes considering both direct path and ground reflection path and uses parameters such as the distance between nodes as seen in the equation 2.3.

$$P_{RX} = \frac{\lambda^2}{(4 * \pi * d)^2} [2 * \sin\left(\frac{2 * \pi}{\lambda} * \frac{h_{TX} * h_{RX}}{d}\right)]^2 * P_{TX} \quad (2.3)$$

Where P_{RX} is the signal power received for a transmission power of P_{TX} ; λ is the signal wavelength; h_{TX} and h_{RX} are the height of the transmitting and receiving antennas and d the distance between them.

Wantanee Viriyasitavat et al. [18], various propagation models for vehicular communications are characterized and categorized. The authors classify the models based on propagation mechanisms they employ and their implementation approach to these mechanisms, and also classify the models based on the channel properties they implement (e.g. environment, vehicle types, placement of transmitting and receiving antennas), while also weighting their complexity in practice. They mention two main approaches in designing models:

- **large-scale propagation:** The large-scale propagation models generally make use of log-distance path loss model and are used for scenarios such as urban intersections, rural environments and highways. As example, the Geometry-based Efficient propagation Model for V2V communication (GEMV2V) proposed by Boban et al. [19] uses different types of path loss models for LOS and non-LOS, namely the two-ray ground reflection model and log-distance path loss, respectively.
- **small-scale fading:** The small-scale fading models, compared to large-scale propagation models, also take in to account effects caused by multipath propagation and Doppler effects due to mobility of vehicles and objects in their surroundings. The GEMV2V model, in small-scale fading, is used in small-scale fading with Gaussian distribution with varying standard deviation depending on the number of vehicles and density of objects in the area.

Depending on the implementation approach and the availability of geographical information, the models are classified based on their implementation approach as follows:

- **Ray-tracing models** require a detailed description of the propagation environment to be able to simulate each scenario and accurately channel statistics.
- **Simplified geometry-based models** take into account the geometric properties of the surroundings, at the same time simplifying geometric calculations by extracting some of the channel statistics either from measurements or simulations.
- **Non-geometry-based (NG) models** mostly follow a recipe: measuring the channel characteristics in a specific environment and adjusting the parameters of the path loss shadowing and the small-scale fading accordingly.

The B2C model falls to this simplified geometry-based model category, because we consider the geometric property of the antenna placement on the bicycle and car. Our model also is a large-scale propagation since we mostly consider LoS scenarios and do not account for the fast fading effect.

2.2.3 Antenna Positioning and Vehicle-Induced Shadowing

These works specifically target the induced attenuation cause by vehicles body in the wireless connections. The signal propagation is attenuated along its path through free space, infrastructures and vehicles. The positioning of the antennas on the own structure they are mounted to should be strategic to harness as much LoS as possible and minimize the attenuation from its own frame.

D. Eckhoff, A. Brummer, and C. Sommer [20], in their work is investigated the impact of different antenna patterns and some interference of urban street and buildings layouts on the outcome of vehicular network simulations. For such, they used 4 antennas with different patterns and ran simulations with such equipment on cars to observe the impact of the orientation of the antennas and the effect of communication's angle. They found that modeling antenna patterns in VANET simulations have a direct impact on their outcomes. They also observe that these networks are highly dependent on line-of-sight in the direction of the vehicle movement for a higher effectiveness.

The authors S. Kaul et al. [8] evaluate the performance of IEEE 802.11a performance by installing five antennas on the rooftop of the car and one inside the windshield. After they have everything setup, they keep a car stationary that emits beacons and increase the distance the distance of the receptor. They have also estimated the radiation pattern for each antenna placement on the car to assess the impact of the car's geometry. From their experiments the authors concluded that: (i) the antenna placement impacts the cumulative link PER performance; (ii) the antenna placement makes their omni-directional patterns more asymmetric and that to keep this pattern the antenna should be mounted at the center of the vehicle; (iii) using multiple antennas can provide 10-25% gains in packet reception rate and 2-5dB gains in received packet RSSI in vehicular networks, since it avoids the effect of vehicle's geometry.

R. J. Weiler et al. [7], the authors investigate how environment induced shadowing influences a 28.5 GHz access link in an urban open square scenario. Shadowing is caused by cars, buses, lorries, and pedestrians passing between the small cell base station and the mobile user terminal. For experimental purposes they have set up two antennas along the side the road and they have isolated typical single shadowing events and provide a model for their description. This double knife-edge model provides a good approximation for pedestrian single shadowing events, however it is not equally applicable for vehicles, because it highly depends on the material each vehicle consists and its size. They also claim that the results show that environment induced shadowing has a significant impact on the path gain and therefore the link budget. The impact of shadowing events depends on the geometrical position of transmitter, receiver and the object causing it. They also mention that the ground reflection has a major impact on the power received from the line-of-sight direction. The shadowing of the ground reflected path can therefore lead to an increase or attenuation of the power received in this direction, depending on the state of the fading effect.

2.3 Discussion and Conclusion

After an extensive research for prior work in this matter, we have come across only a few papers that refer to bicycles that are incorporated in vehicular network. For this reason we have looked to works that include scooters, since they have many similarities compared to bicycles, and also looked at some wireless technologies applications that we can relate to.

The thesis differentiates from others work through the inclusion of bicycles in vehicular networks, characterizing the link between bicycles and cars (throughput, PDR, IRT) and RSSI propagation. From these contributions, we highlight some aspects that shaped our considerations for the matter of this thesis:

- **antenna positioning:** the bicycle's body has an impact on the communication, and the performance varies according to where the antenna is placed, being the furthest possible mounting point from the ground one important aspect.
- **human-body shadowing:** the body of the cyclist body also attenuates the transmitted signal and we will have it in consideration in our experiments.
- **scenarios:** from the literature we have learned that the scenario of intersection between too vehicles, with and with out obstructions like vehicles and other urban elements it is widely studied and considered a big motivation for the development of safety applications to prevent collisions.
- **IEEE 802.11b/g:** for this thesis we have decided to use WiFi as the wireless technology for its easier accessibility through off-the-shelf products and big presence on mobile devices and structures, and more recently, the inclusion of WiFi hotspots in cars.

Chapter 3

Experimental Characterization of 802.11 Vehicular Radiation and Path Loss

We describe the experiments that we have conducted to populate our B2C model with the necessary data. These experiments were carried to support the proposed model, and validate it in the next Chapter 4 through simulation of selected scenarios of interaction of a bicycle and a car. At the end of each experiment we note the learning outcomes and remark a more personal comment regarding the experimental procedure and its learning process. The approach we followed is described next:

1. We decided to first test and evaluate what would be the most adequate mounting position for the antenna on the bicycle (in Section 3.2).
2. We measure the (inhomogeneous) signal radiation around the bicycle for selected antenna positions with a rider mounted to it (in Section 3.3), to gather data for the component L_B of our model.
3. We measure the (inhomogeneous) signal radiation around the car, in Section 3.4, informing us about the shadowing caused by the car's structure and other elements within it (e.g. edge pillars, seats) and feeding the component L_C of our model.
4. An evaluation of received signal strength with respect to distance without obstructions and for a large distance (400 meters) was also done to characterize the element L_{free_space} , in Section 3.5.

We then emulate the scenarios and compare the obtained RSSI values with our proposed model, described with greater detail in the following Chapter 4.

Parameters for wifi	Values
Tx power	20 dBm
Nr Retries	2 (default:7)
Beacon bit Rate	1 MBits/s
txqueuelen	10
channel	4

Table 3.1: Configured parameters for the wifi antennas

3.1 Common Experimental Setup

Throughout the experiments described in this chapter, the following experimental setup was used unless clearly noted. The used antennas are TP-Links TL-WN722N [21] which have a detachable omni directional antenna with a RP-SMA connector to the board that contains an Atheros AR9271-AL1E chip and an USB interface. These antennas rely on IEEE 802.11b/g standard and are to be attached to various locations (e.g. inside the car, on the bicycle, tripod stands) connected to our portable PCs and either configured into monitor mode or ad-hoc mode with the parameters described in Table 3.1. The nominal throughput in the IEEE 802.11b/g standard can take a value from a range of pre-defined values. The actual value that is used is decided in on-the-fly negotiation between the two nodes. The 'b' and 'g' variants achieve a range of nominal throughput, namely 1, 2, 5.5 and 11 Mbit/s for 'b', and 6, 9, 12, 18, 24, 36, 48 and 54 Mbit/s for 'g'. These are achieved by means of different modulations and coding rates (from BPSK-1/2 to 64-QAM-3/4). Link-level reliability is assured by long-packet re-transmissions, limited by default to 7. Experiments with the car, the Volvo XC90, we also have used the GPS tracker Globalsat BU-353-S4 [22] to record the positions for measuring distances between the bicycle while it is moving and then process all the information a posteriori.

3.2 Study on antenna positioning on bicycles

In this section we describe the procedure for the carried experiments on radiation patterns for antennas mounted on different places on a bicycle. We want to find out what is the impact of the bicycle's body on WiFi communications. For such, we have selected different antenna positions to observe the impact of bicycle's geometry in the transmission power for the communication. The selected antenna positions are as follows (Figure 3.1a):

1. Middle of the handlebar - is the most common location for placing cycling-support gadgets, such as smart phones and performance meters. From an antenna perspective, this location offers little shadowing as few bicycle elements are at the same height;
2. Under the rider's seat - this location is an opportunistic place due to its free volume, supports gadgets and pockets that can be installed under the seat. It is an open and reasonably protected space, and is not close to objects performing large movements;

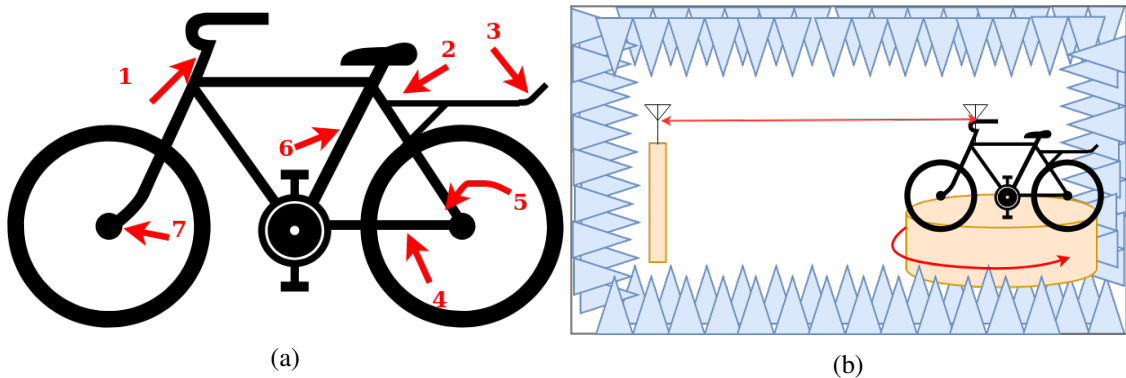


Figure 3.1: (a) Selected antenna positions for the link characterization, namely 1) handlebar, 2) under seat, 3) back rack, 4) back wheel, 5) chain side of back wheel, 6) inner frame, 7) front wheel and (b) Depiction of anechoic chamber setup with rotating platform under the bicycle

3. In the bicycle's rear-end - many bicycles feature a back rack (or can be added a posteriori) for carrying additional loads. From a propagation stand-point, its far-end offers no obstructions towards the back and sides of the bicycle;
4. Next to the back wheel (vertical and horizontal polarization) - the bar between the axes of the back wheel and of the pedals, on the side opposite to the chain, provides an unimpeded, horizontal volume where an embedded device can be installed. The antenna is close to moving objects (e.g., legs, wheels);
5. Chain-stay - similar to the previous position, but on the chain side. In this case, the antenna is also close to the chain system (i.e., chain, crank set and cog set). This position is motivated from a product design perspective, as numerous commercial products use the space within the chain to store embedded electronics, e.g., batteries, dynamos, communication devices (often within a protective encasing);
6. Inside the bicycle's frame - the interior of the frame diamond is used very often to place support objects (e.g., water bottles and pouches). However in the communication perspective, it is a region around which there is considerable leg movement and the shadowing may be substantial;
7. Next to the front wheel - similar to the back side, attaching to the axes of the front wheel. It presents a opportunistic place although is close to the moving wheels.

In short, the mounting points were chosen given their already commonly used positions for products and gadgets, commodity, and also for a opportunistic usage of the bicycle's body.

3.2.1 Experimental methodology

The experimentation to be described is what we have used to obtain RSSI values for the radiation pattern of different antenna mounting point on a bicycle. We carried out the measurements at the

anechoic present at the Faculty of Engineering of the University of Porto. This anechoic chamber has two stands for the antennas, apart by about 4.5 meters. One of them has a motor integrated to provide rotation and the other can have its height adjusted. On this rotating stand, we have mounted our bicycle with the antenna attached, and this way, by rotating the whole structure we can make an analyzes of the radiation pattern for each antenna placement on the bicycle. Each antenna is connected a cable that passes to outside the chamber so we can connect the antennas to computers. Outside the chamber is where we manage the experiments through the computers. The antenna on the fixed stand was considered the receiver and this wireless interface was set to monitor mode, so it would inform us of the RSSI value for each beacon packet from the emitter, which is configured in the Ad-hoc mode. The emitting antenna was set up and attached to the bicycle to one of the 9 selected positions. The rotating platform was so close to the chamber's wall that we had to remove either one of the wheels to not damage it and freely rotate the bicycle. Each session would take at least an hour because each measurement for each angle (out of 72) would take 40 seconds, plus the mounting and amounting of antennas and the bicycle. The whole setup is depicted in Figure 3.1b. The setup of the bicycle for each position of the antenna is shown in Figure 3.2. Once we have placed the antenna on the bicycle, we would have to setup the interfaces with the parameters from Table 3.1.

There are measurement scripts running at the laptops serving as TX and RX, and a MATLAB script running in a third computer to coordinate the rotation of the stand and the measurement sessions. We would run the scripts that allow us to make the measurements. The room's computer allows us to run the scripts and then rotate the platform that our bicycle is standing on. It would repeatably do this until it has rotated fully in a circle.

These scripts had a transmitter side and a receiver side:

- The receiver side would use the iwlist program to scan for the transmitter ad-hoc's beacon signal, and measure its RSSI.
- The transmitter would connect to the receiver and after a pre-defined time, it would close the connection and just wait that the receiver measures the RSSI beacons.

The procedure for the experiment followed this sequence:

1. Attach antenna to a position on the bicycle
2. Setup bicycle on rotating platform in the anechoic chamber
3. Center the attached antenna to the center point of rotation
4. Adjust the other antenna's height that is on the pedestal
5. Verify that bicycle can rotate freely all around
6. Configure antennas WiFi's parameters (Table 3.1)
7. Start measurement scripts

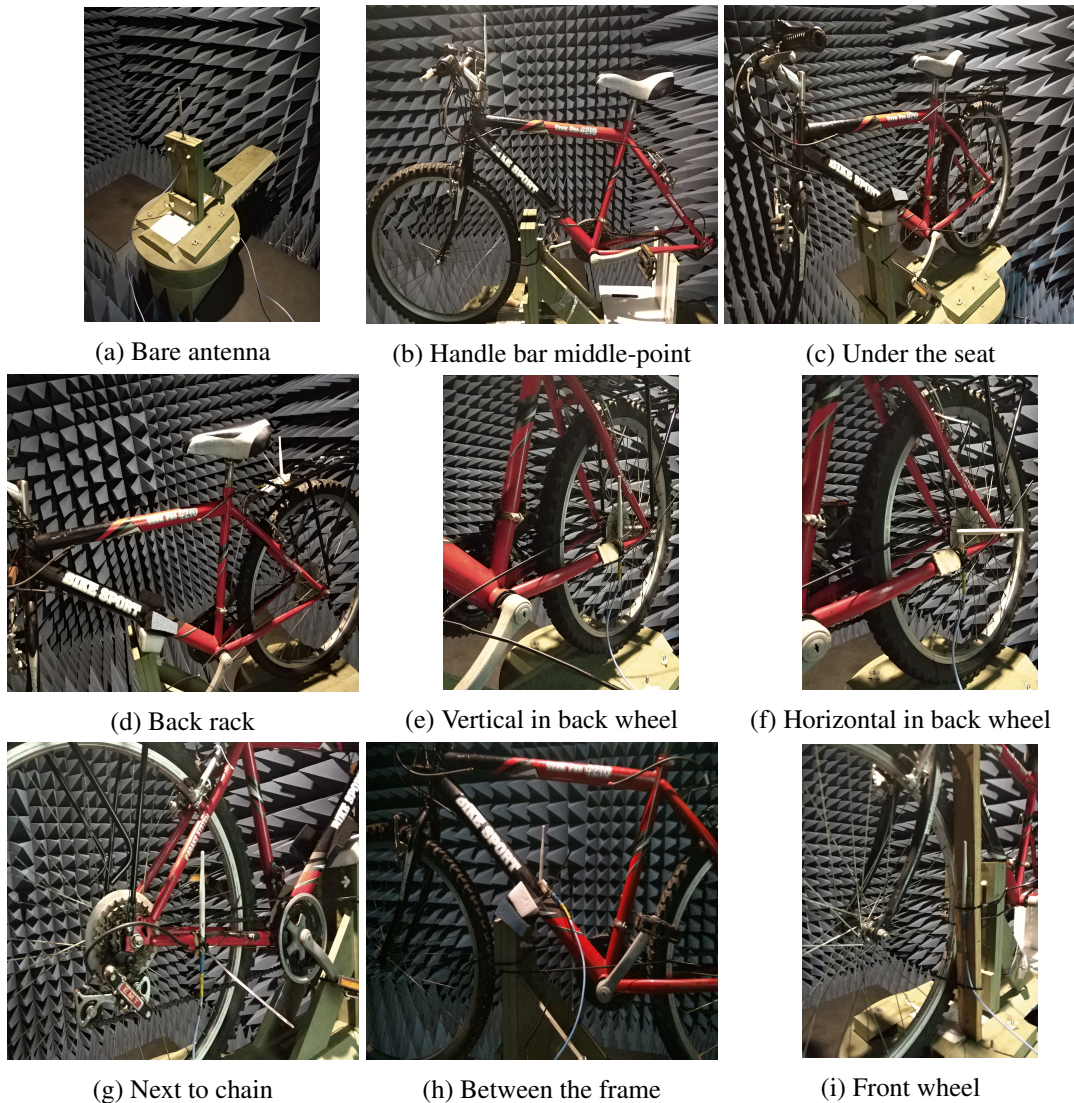


Figure 3.2: Antennas setup

8. Save measured samples once it has completed the session

Then this process would be repeated for all the desired placements of the antenna on the bicycle.

3.2.2 Results

In Fig. 3.3 it is represented the obtained RSSI pattern around each antenna position on the bicycle through polar plots. In these plots the center of the circumferences represents our bicycle which is facing upwards. Starting from 0 degrees, each angle around the bicycle has a step of 5 degrees and rotate clockwise. This is a rough approach to a radiation pattern, but it is scaled to allow us to effectively compare each diagram with each other. Each point represents the average RSSI value recorded for that angle in relation to its maximum value (0 dB).

These are the observations from each antenna position:

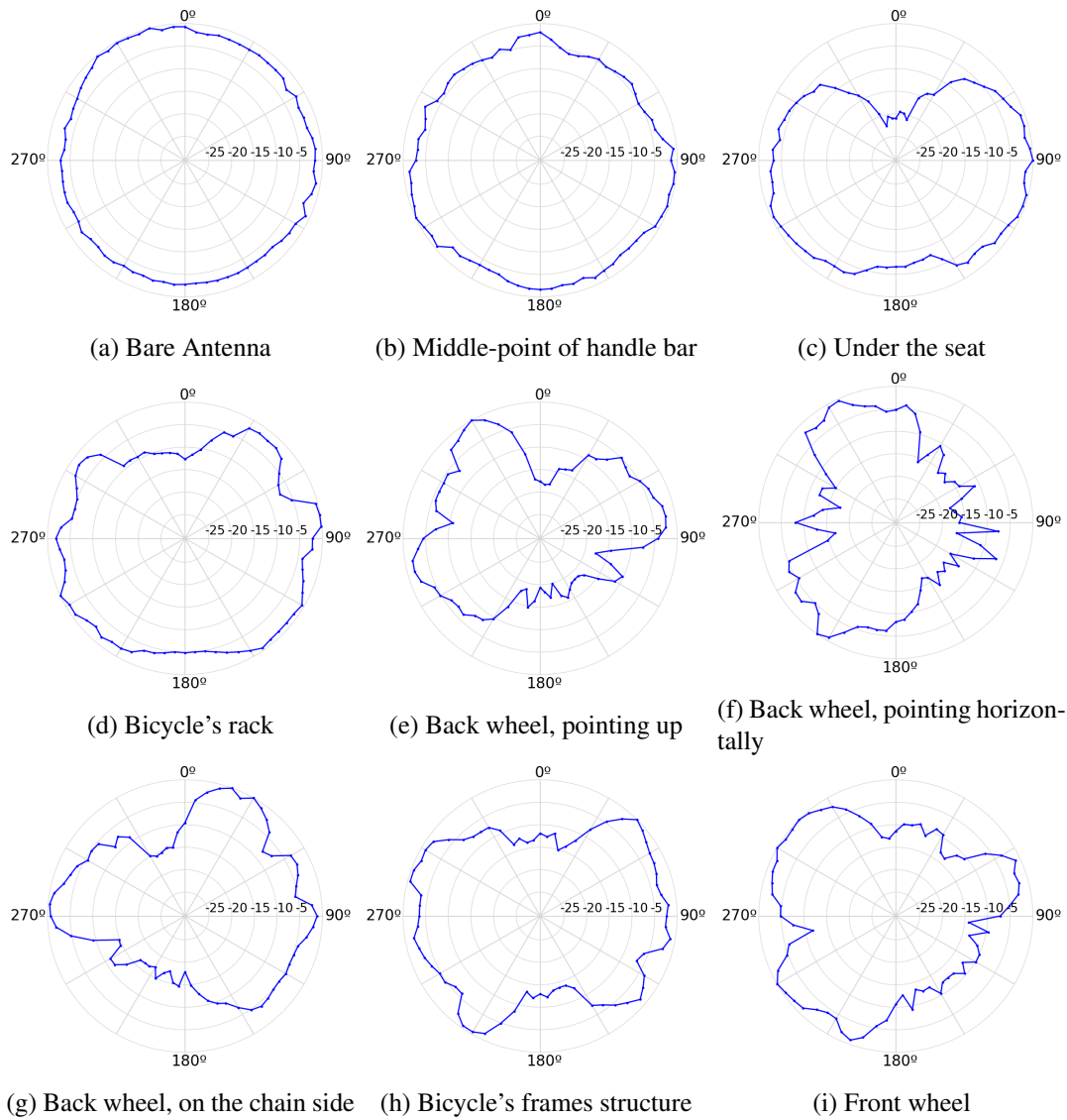


Figure 3.3: Antenna's RSSI pattern over different mounted positions on the bicycle, which is facing to 0 degrees

- (a) To better understand how the bicycle frame impairs signal propagation, we have also measured the radiation pattern of the bare antenna for reference.
- (b) The middle point of the handle bar is an intuitive place for the antennas, and has been proven to be rightfully so, because it is mounted on a tall place of the bicycle and there is not much material in its way. The results show a round pattern with low interference all around. According to the paper [14], on the furthest point from the center of the handle bar would be even better, but there was not enough room to install it there;
- (c) Under the seat, although that is a very opportunistic use of space, we can see that in Fig.3.3 it lacks in communicating with anyone in front of the bicycle due to its frame attenuation of about -20 dB upfront;

ANTENNA POSITION	AVERAGE STD DEV	AVERAGE RADIUS	AVG DISTANCE TO RADIUS
0 JUST ANTENNA	0.77	-48.21	0.10
1 HANDLEBAR	0.70	-45.91	0.17
2 UNDERSEAT	0.75	-52.01	0.73
3 REAREND	0.74	-47.86	0.37
4a BACK (vertical)	1.05	-50.89	0.71
4b BACK (horizontal)	1.03	-52.77	0.62
5 CHAIN SIDE	0.96	50.19	0.73
6 INNER STRUCT	1.23	-51.32	0.53
7 FRONT WHEEL	1.15	-53.024	0.54

Table 3.2: Statistical values from results data

- (d) On the bicycle's rack is similar to under the seat but it is less obstructed for communications in front of the bicycle and has a better overall performance too, with a attenuation of about -5 dB on backwards and -13 dB forwards;
- (e) and (f) In general both are not very effective, although it was interesting to see what happened if we changed the orientation of the antenna. We can observe that antennas radiate in a plane perpendicular to it, it is intuitive that the horizontal antenna has a better RSSI value on the front and the back of bicycle and bad on the sides, while it happens the opposite to the vertical alignment of the antenna;
- (g) This position is similar to the previous one, we can notice on the results how symmetric it is to (e) and that the wheels of the bicycle greatly influence the quality of the link, it lacks signal strength from angles 180° to 270°;
- (h) When we considered this position for the antenna, intuitively, we expected for it to not have a very good performance but it is quite similar to the others, being not affected on the bicycle's sides while having an attenuation of about 13 dB on the front and back, and it also has a good, practical and not intrusive spot to install the antenna;
- (i) This place is similar to (e) and (g), which we can notice a great impact of the wheel in the communication process, greatly attenuating the signal from 90° to 180°;

The criteria we will use to select a subset of positions to use in subsequent experiments is the similarity to an isotropic pattern – in other words, how 'round' is the pattern. The objective metrics we identify to evaluate this 'roundness' are: average std. deviation, average radius, and average distance to radius. The Table 3.2 has the results for such metrics of the data collected of RSSI values for each position.

3.2.3 Discussion on Quality of Antenna Positions and Final Remarks

The purpose of this experiment was to observe the impact of the bicycle's geometry on wireless communications through different the positioning of the antenna. This study will also inform about positions to be used on further experiments. From the results we observed how RSSI was affected by the antenna position and based on our criteria we chose what we considered the most adequate deployment of the antenna. The best characteristics and behavior of a mounting position for the antenna is one that has a consistent and low attenuation levels of RSSI that is transmitted. The more the average of each angle samples approximate to the average of all angles, the better. The physical intrusion of the antenna is also considered: it should interfere with rider the least possible. For that matter we have made measurements in the anechoic chamber and considered, through the obtained results, that the most appropriate mounting points would either on the handle bar or on the back rack, which both will be carried for the following experiment in Section 3.3.

On a personal remark, these experiments were quite demanding, during this procedure we have faced several challenges that may have influence the experiments, namely

- due the rotating platform was so close to the chamber's wall the vehicle wheels had to be removed to avoid damaging to the chamber isolating material, while also being able to center the bicycle;
- These experiments were very time consuming as mentioned, each session would take at least an hour, and given the anechoic chamber access was fairly limited, the time constraints were more demanding;
- In some sessions, they just went wrong. Due to some human factor such as wrong configurations or malfunctioning of the scripts, some results were withdrawn because they were not reliable, increasing time consumption;

3.3 Bicycle-cyclist Shadowing

Our proposed model considers as one of its components the impact of the cyclist-bicycle system as one entity, so we want to feed the L_B element with reliable data with the presence of a human body. The previous experiments gave us some information about the performance of the WiFi signal due to its antenna position on the bicycle, but the human body was not taken into account and could lead to less accurate predictions of our model.

It was decided to do measurements with a rider and without one, so we could compare both experiences to observe such impact, for three selected antenna positions:

- **Middle of handle bar:** we made measurements with this placement because it was the most promising antenna position from the results extracted from last experiment (in Section 3.2).
- **Back rack:** this place was also picked from the previous experiment (in Section 3.2) due to its consistent and reliable performance of the RSSI values. On the other hand, in this

scenario, the antenna could be pushed even further to the back of the bicycle, since the space was limited in the anechoic chamber and it had to be more centered on the rotation point, providing less obstruction caused by the bicycle's frame.

- **Left grip of handle bar:** according to [14] the higher the antenna is and the furthest it is from the center of the vehicle body (where they have used a scooter) the better. We believe this position is similar to the middle point of the handle bar, but might be more effective than the middle point in co-linear cyclists, while on the other hand it is more intrusive where it is mounted.

3.3.1 Experimental methodology

In this experimentation, similarly to what is described in Section 3.2.1, we intend to obtain the RSSI values around the bicycle, with and without a person sitting on it for various angles. A better-suited measurement location (such as the anechoic chamber) was not used due to practical constraints: the measurements were carried out in an outdoor setting due to the logistic difficulties in having a person riding the bicycle in the anechoic chamber (as the rotating stand could not support it). In these new conditions, we also opted to sample less angles (16) to keep the experiment time within reasonable limits.

We performed the measurements in FADEUP's athletics field (41.1781292, -8.6049907), where there was enough space to make measurements of a 5 meters radius, with the presence of some vegetation and trees, no buildings but a few football's goals, low interference from other WiFi access points, few people that can obstruct the procedure and the floor was made of tartan which is used to make the athletic running track. Doing the experiment would be more precise, efficient and quicker and less interference vulnerable inside the anechoic chamber but we could do such without damaging it and its equipment. In the field we could have someone sit on the bicycle but it is more prone to interference from other sources or reflections, such as the radiation reflected on the floor.

For setting up this experiment we have used the help of four camera tripod stands to hold antennas connected to laptops. We had set up one of each of these stations around the bicycle, for a radius of 5 meters, of 90 degrees apart from each other. After each session, the bicycle would be rotated by 22.5 degrees. In the end, we have covered angles around the bicycle with a step of 22.5 degrees. The diagram Fig 3.4a illustrates 4 rotations, and each rotation contains RSSI measurements of the angle from the bicycle front to the tripod. Figure 3.4b depicts the dedicated measurement equipment and its setup environment.

Each session would compose of running the measuring script on each laptop. The antennas mounted to the stands were configured in monitor mode and run a script that would register the RSSI values of beacons through `tcpdump`. The bicycle had a antenna mounted to the desired position that would be connected to a laptop, which would be configured in Ad-hoc mode, with the same set of parameters as stated in the Table 3.1. The transmitted beacons by the bicycle would

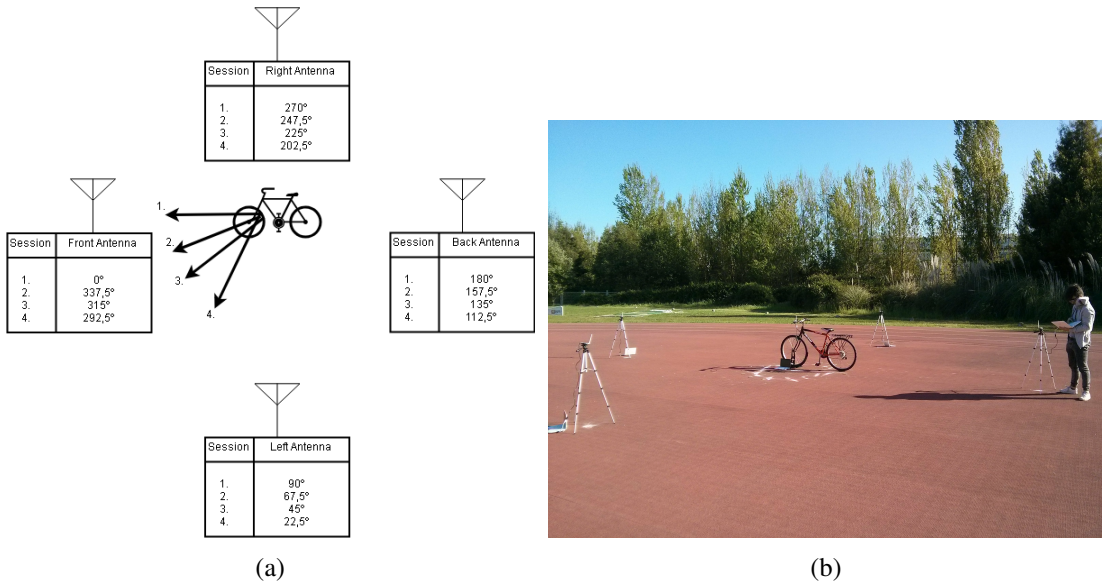


Figure 3.4: Experimental setup used for human shadowing experiment. (a) The bicycle is centered to 4 tripods in a 5 meters radius with antennas mounted. After a capturing session, the bicycle will rotate 22,5 degrees, which will have a new angle perspective from each. At the end of 4 rotations the samples will have 16 angles captured with a step of 22,5.

then be captured by each antenna on the stand. After capturing, all the logs captured from each PC are stored, for later to be sorted and processed.

The procedure for the experiment consisted of the following sequence:

1. Attach antenna to a position on the bicycle
2. Setup bicycle in the center facing the stand without the rider
3. Configure antennas WiFi's parameters on every laptop
4. Start scripts that captures RSSI samples, on each laptop
5. Once every computer has captured, have the cyclist sit down and rerun the same scripts
6. Then we rotate the bicycle according to the markings and repeat the process

This whole process then would be repeated for all the remaining antenna placements.

3.3.2 Results

Figure 3.5 presents the obtained RSSI pattern around each antenna position on the bicycle comparing the attenuation of the presence and absence of a rider. In these plots the center of the circumferences represents our bicycle which is facing upwards. Starting from 0 degrees, each angle around the bicycle has a step of 22,5 degrees and rotate clockwise. Each point of the plot, is the mean RSSI value of captured samples for that angle in relation to the maximum of all other angles.

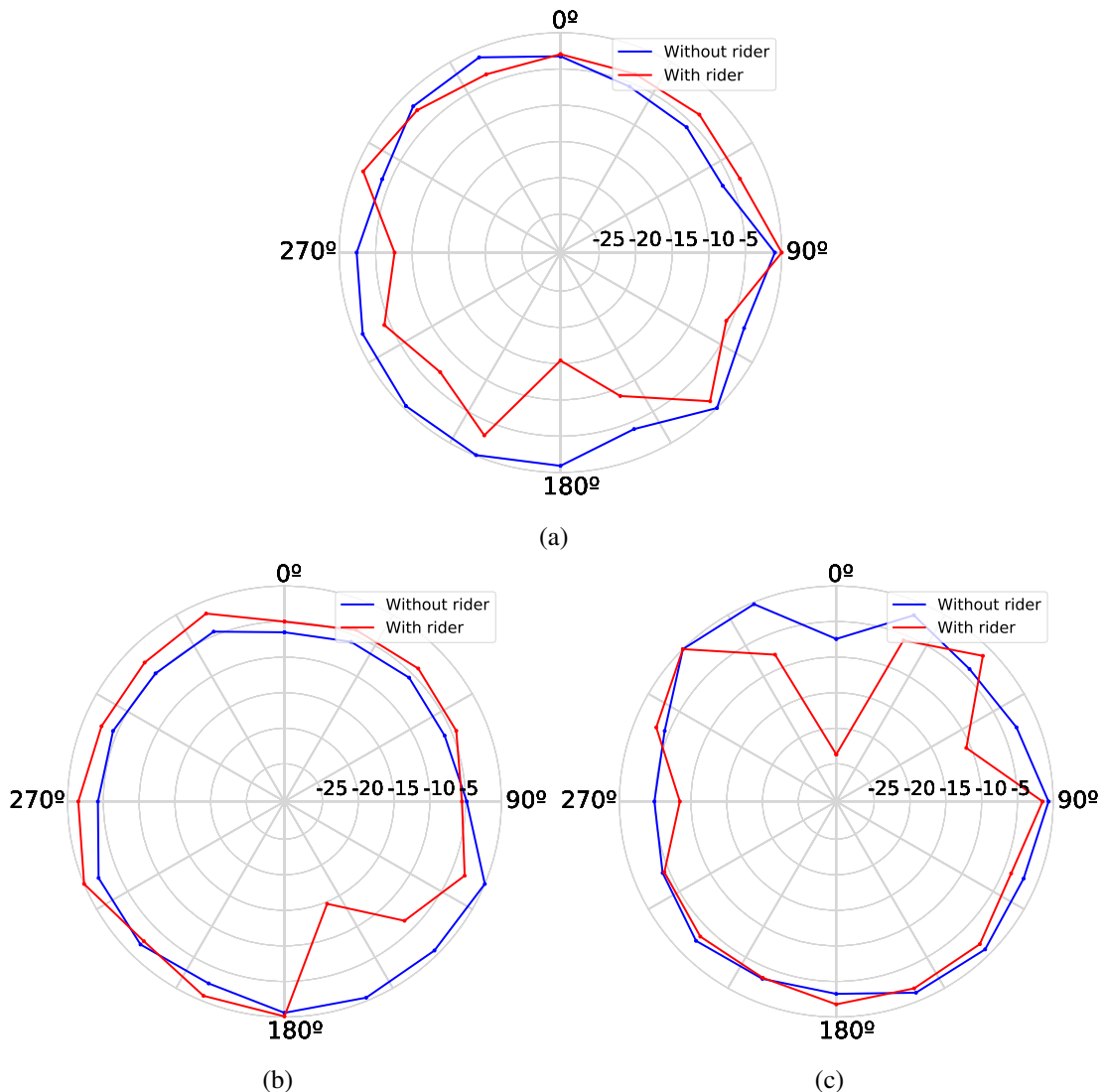


Figure 3.5: Antenna's RSSI pattern over different mounted positions on the bicycle, which is facing to 0 degrees, with and without a rider: (a) middle point of handle bar (b) left grip of handle bar (c) bicycle's back rack

The results depicted in Fig. 3.5 demonstrate that the human body actually does have great impact in the link quality, we can observe that it can attenuate the signal for about -15 dBm in the angles in which we observe the greatest variance:

- In the handlebar we can observe the human body attenuation of 15 dBm on 180 degrees to when compared when the rider is absent because it obstructs the signal to the way backwards. We can also observe some attenuation at 270 degrees due to the arms positioning of the rider, which demonstrates some sensibility of the signal to being affected by the arms and not only with a big area such as the torso.
- At left grip it is mainly attenuated in the opposite side since the human body is in the way, at a range of angles from 135 to 180 degrees, when compared to the absence of the rider.

Some of the attenuation caused from 110 to 135 degrees is due to the presence of the arms that are grabbing the handle bar.

- (c) in the back rack position we can observe it is not fit for links in the front of the cyclist, its body attenuates the signal by about -15 dBm, and in this case it was affected by the rack structure to some angles (e.g. 270 degrees and 67.5 degrees), affecting by about -5 dBm.

3.3.3 Remarks and Discussion on Antenna Positioning

These results from this experiment were somewhat expected and have provided data for the model, the L_B component for a set of three positions that include the attenuation caused by the human body. We have concluded from the results that:

- communication to the front is greatly impaired by the human rider in the back rack antenna position, but we could argue it offers the least intrusive position.
- the antenna next to the grip is less impaired by the human body but it is not very practical due its location on the bike.
- the antenna on the middle-point of the handlebar is what we considered best due to being less intrusive to the rider and easier to install while being more effective in the direction that the bicycle is facing while moving.

While we have data to that makes up the L_B component for the three antenna positions, we will carry further experiments using the middle-point of the handle bar as the mounting point.

To carry out this experiment was quite a challenge due to time constraints and places to do it. The anechoic chamber would save quite some time, but it is not feasible to have anyone to sit on top of a bicycle through a long period of time, without damaging the anechoic chamber too. Apart from occasional script bugs, the windy but sunny weather made it a bit more tough because it was making the stands fall, and we were exposed for few hours to the sun.

3.4 Car Shadowing

One of the parts for our model is the L_C component which consists of the attenuation caused by the car's body. Thus we capture a radiation pattern around a car. Having access to a car with an incorporated WiFi AP, we captured the RSSI pattern for its production WiFi equipment (PE) and have this equipment compared with our own setup (DME), which is further detailed in a later chapter (Chapter 5) in a series of captures of representative scenarios. This way, we can cover a bigger range of scenarios and applications and help prevent many dangerous cases that involve a car hitting a cyclist, while also making an opportunistic use of already existing implementation and exposing other possibilities . Since we don't have direct access to such built-in system to configure it at our will, we will measure its emitting signals and map the PE behavior to our DME and evaluate our system to a commercialized one. To test such, we have looked for a place with

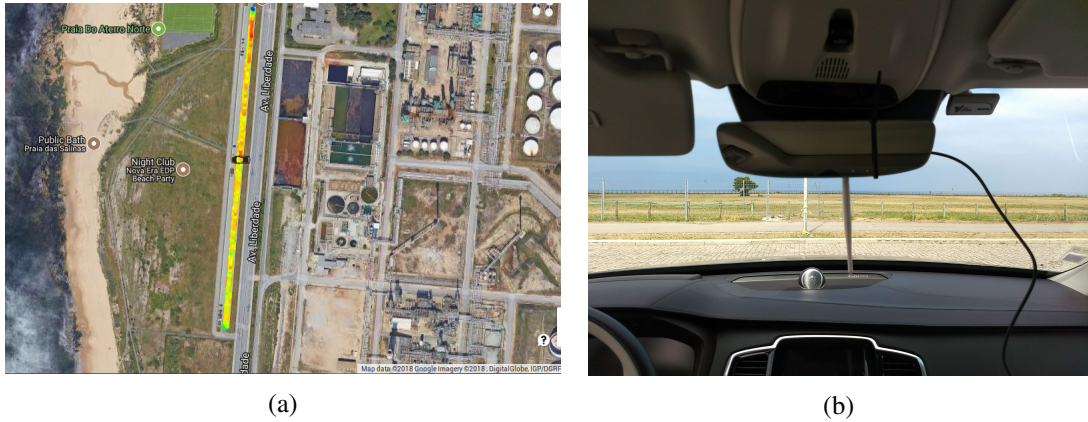


Figure 3.6: (a) Experiment location and (b) antenna setup in car

few cars present to reduce interference, we went to a parking lot in Leça de Palmeira (41.21668, -8.71309) - see Figure 3.6a- and set up our experiment there. We didn't have access to a large anechoic chamber that could contain the car and rotate it therefore we have considered the vehicle to be symmetrical in its width to require less capturing time and have only captured half around the car.

3.4.1 Experimental methodology

In this experiment we intend to obtain and compare RSSI values around the car from its built-in system and our own DME. We did not manage to prior identify where the PE antenna is implemented, so we decided that a common and intuitive place to mount the antenna would be at the rear-view mirror, as it can be seen in Fig 3.6b. Later on, we have learned that it is located in the back of the car (see Fig. 3.9), but at that time we did not know that, which led us to install the antenna at the rear-view mirror. On the other hand, using our setup allows us to: make throughput tests; change data rate, which car's AP has a low frequency of beaconing (1 beacon every 100ms); this location provides a better link quality in front of the car, which is most useful for security reasons involving crashes.

Our experimental setup is similar to the previously mentioned on other experiments. We set up two bicycles with a laptop, a GPS tracker and a antenna, and walked them back and forth in a straight line up to 100 meters, sampling RSSI values of DME and PE, with the antenna always facing the car to avoid the bikes structure to interfere with the RSSI values, maintaining LoS at all time. We have made two measurements at each side at a time. We have chosen to take this approach to the measurements because if the car's antenna is mounted on top of the car, any communication near the car can be affected by its own structure. We tried to measure through various distances to also vary the vertical communication angle, as is represented in Figure 3.7a.

To measure the PE's AP signal, we had just turned its hotspot on and measured the power and reach of its beacons with the antenna mounted to the bicycle in monitor mode through the script also used previously in Section 3.3 that makes captures using tcpdump, with the adjust that we had to stop it so we could stop recording on demand (oppose to defining a timer). Then, similarly, with

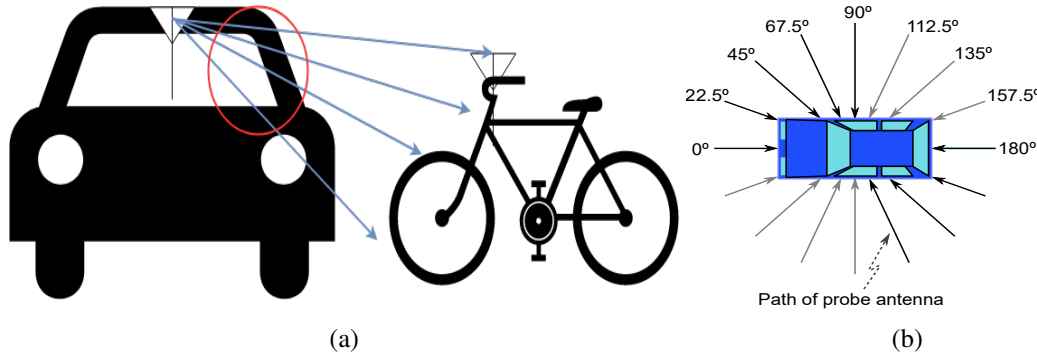


Figure 3.7: (a) Depiction of vertical angle interference in communication and (b) car radiation pattern captured angles from experimentation

a antenna connected to a PC in the car configured like mentioned in Table 3.1 in ad-hoc mode, apart from being in channel 6 to match the PE channel, and measured its beacons using the same script.

The procedure for this experiment would be repeated for each angle through the following steps:

1. Positioning car to the desired angle and the bicycle 100 meters apart to start the session
2. Perform adequate configurations on available laptop
3. Start the script and walk the bicycle towards and backward the car, always facing it
4. Do three runs of walking
5. Stop the script
6. Change setup and repeat process for the same angle

With this method we have obtained 9 angles, with a step of 22,5 degrees from 0 to 180 degrees for PE and DME, as depicted by Figure 3.7b. As mentioned, due to time constraints and that we wanted to test both systems, we have considered that the car is symmetrical to its width, so this way we consider to have covered angles all around, from 0 to 360 degrees with a step of 22,5 degrees, mirroring the results.

3.4.2 Results

Having captured RSSI samples around the car, we have designed a rough estimation of the in-vehicle 802.11 antennas radiation pattern for the DME and PE setups. Figure 3.8 presents the results from what we have sampled through the various angles and distances. Each data point represents the normalized average RSSI for a given angle and TX-RX separation. The normalization is performed by subtracting the maximum average RSSI value (i.e. -35.76 dBm for DME setup with angle 0 and 10 m bin) from all remaining measurements. The standard deviation of the measured RSSI values (right side) exhibits large deviation at short distances specially at the

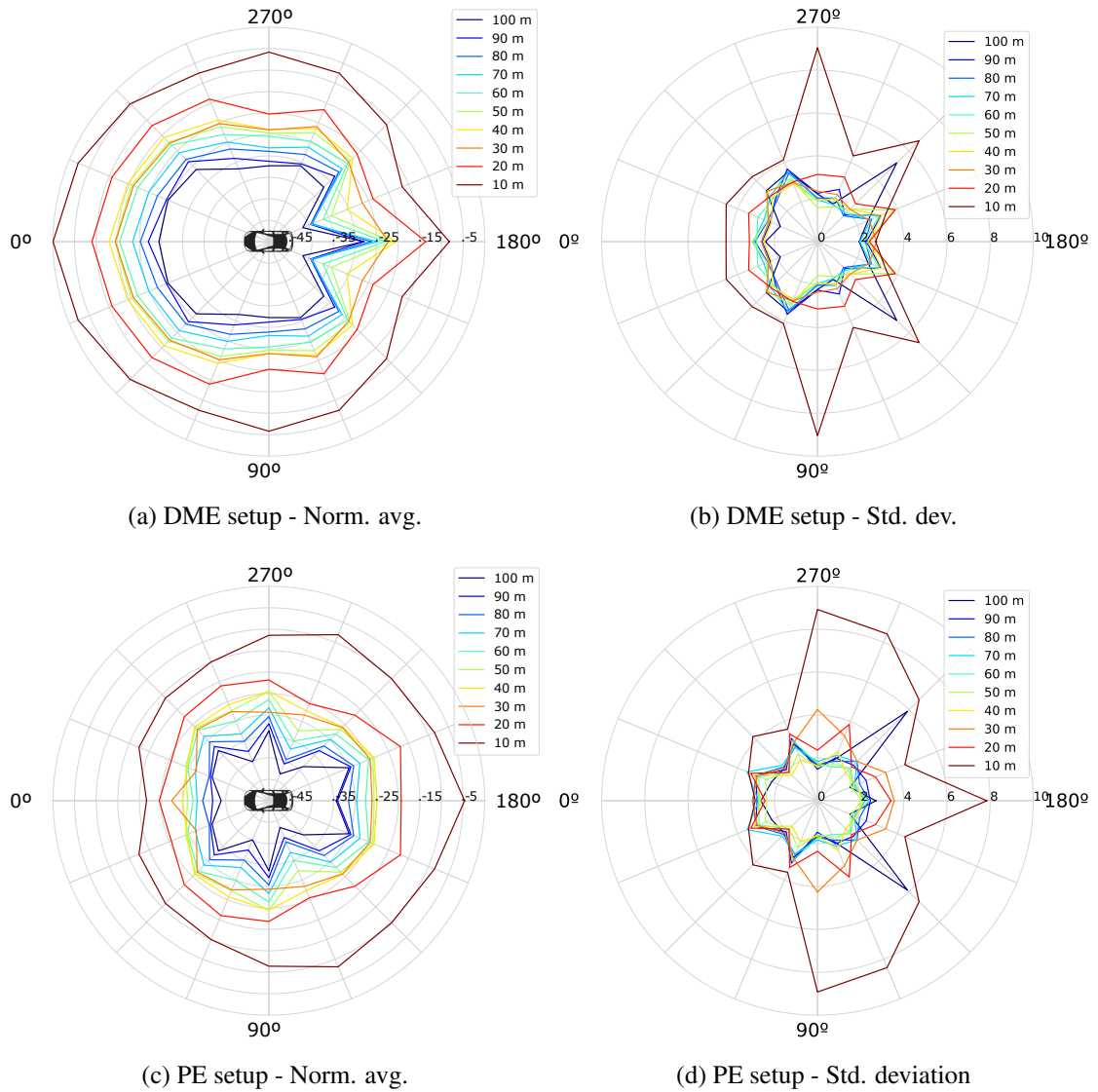


Figure 3.8: Normalized average RSSI (left) and standard deviation (right) of measured RSSI for the DME and PE setups installed in the car, and different TX-RX separations. The vehicle's front is aligned with the angle 0

angles 90 and 270 in both setups; in the PE setup also large deviations occur for communications towards the back of the vehicle. In general, this metric decreased progressively for larger TX-RX distances.

The presented results show that - for both setups - the transmitted signal is considerably impacted by the car's body. We argue that it mainly occurs due the vehicle's elements (e.g. pillars) that impair signal propagation to outside of the vehicle leading to more pronounced shadowing. For a given distance, the average signal attenuation can vary for the considered angles between 6.4 to 17 dB (DME setup) and 12.1 to 20.9 dB (PE setup). The results also suggest that, for a given angle and setup, the level of obstruction varies for different TX-RX distances due to increased shadowing caused by additional obstructions, for instance, due to the lower height of the bicycle



Figure 3.9: (a) Side-view of the test car including location of the in-vehicle antennas for the dedicated measurement equipment (1) and production equipment (2) setups (b) The production equipment antennas is located under the shark fin of the car.

antenna. For instance with the PE setup, the pattern is fairly omni-directional at low TX-RX separation while a more star-like pattern is evidenced for higher node separations. Comparing both setups, we observe that in general the DME setup favors propagation to vehicle’s front, while the PE setup favors propagation to the vehicle’s back and, at higher distances, also to perpendicular directions (i.e. angles 90 and 270). The greater signal response in the back of the car with the PE setup , indicates that the car’s WiFi antenna is mounted below the shark’s fin antenna in the rear of the vehicle (see Fig. 3.9), as opposed to DME setup, center of the rear-view mirror. As expected, the distance between the isolines sharply decreases with the node separation due to the exponential decrease of the transmitted signal strength.

3.4.3 Conclusion and discussion

In this experiment we tried to characterize the RSSI patterns around a car, using its own built-in WiFi hotspot and the setup we have used so far. We have done this by measuring the signal's RSSI at various distances, while also varying the angle by rotating the car after every session. These results provided us the missing piece to our model, the L_C component, now we have a pattern for the cyclist-bicycle radiation pattern(Section 3.3) and the car radiation pattern, to be proven to proof in the following Chapter 4. This experiment also provided us an insight to the different performances for two possible locations to install WiFi antennas and the quality of the link for two different setups, a off-the-shelf equipment that is easily obtainable compared to a commercialized product used for a different end. This is further discussed in Chapter 5 As for the experiment itself, it went through some technical difficulties where we could barely use one of the setups on the bicycles due to sample capturing malfunctioning and during the logs analysis we have came upon GPS errors which have been rectified. Other issues include the movement through the street where occasionally we would have people and cars passing by, which could interfere with the results.

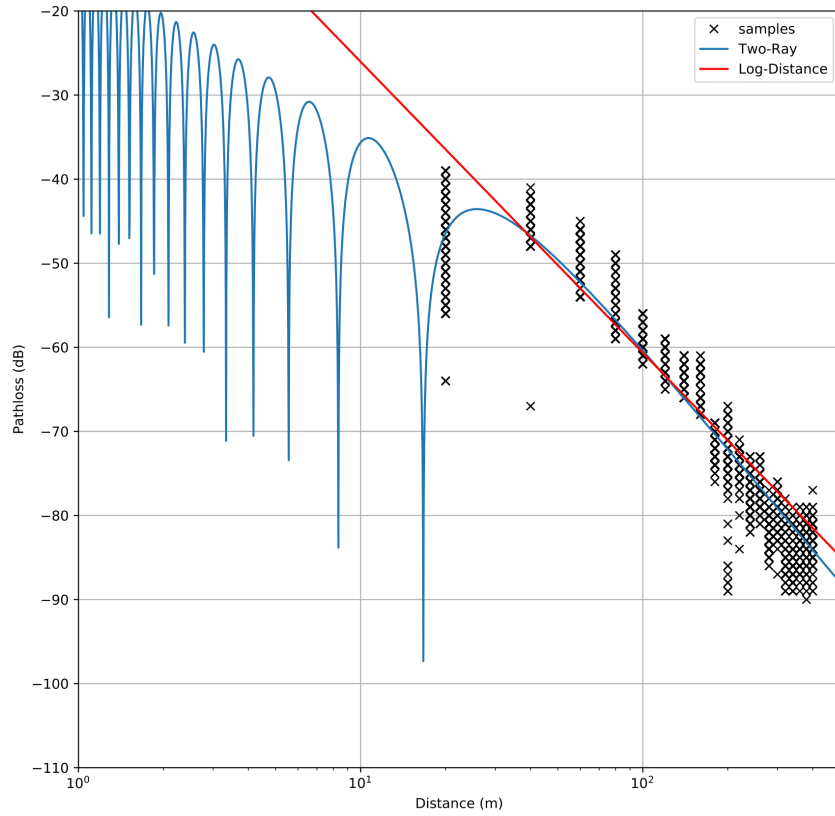


Figure 3.10: Measured data, and fitted log-distance and two-ray ground models.

3.5 Path Loss Evaluation

As a necessary experiment for validating our model we made this experiment to collect data for the path loss model with the antenna we were using, more precisely the L_{free_space} component in our model which results were to be obtained empirically. This experiment we will show how much power the emitted signal from our antennas is lost through increasing distance between two antennas, as the Log Distance Path Loss model suggests. We went to the parking lot in Leça da Palmeira (Fig. 3.6a) and used our DME. We deployed 2 camera tripod stands and laptops connect to antennas mounted on these stands. With the help of measuring tape we would measure 20 meters apart from the beacon emitting antenna and place the receiving end, followed up by running the scripts which contain tcpdump. We have repeated this process 20 times, collecting data every 20 meters up to 400 meters.

Figure 3.10 it is represented the RSSI values we have sampled over different points of distance between TX-RX. The black crosses are the values of RSSI captured to its corresponding distance. The red line is the Linear Regression of the captured RSSI values, which can be described through the linear functions parameters m and b ($y = m * x + b$). The values are such that:

- $m = -3.46181627$
- $b = -36.46546972$

These values make part of the Long Distance Path Loss model which constitutes the component L_{free_space} , being: $\alpha = m$, $P_0 = b$ and d_0 , the reference distance, = 20.

Along side, the blue line is the representation of the Two-Rays Ground Reflected Model which is a theoretical model for path loss that also considers interference reflected from the ground and it is also commonly used for describing the attenuation of signal through free space path loss in vehicular environments. The Equation 2.3 takes parameters such as: λ is 0.12; h_{TX} and h_{RX} - the tripods used were 1 meter high; and P_{TX} and P_{RX} the power of the transmitted power is 20 dBm.

We can observe that at greater distances both models have similar approximations of our samples but the two-rays path loss model seems to have greater precision when the two antennas are nearer to each other. Under 20 meters the linear regression of our samples gets positive values for smaller distances which is inconsistent with reality. Although we were limited to measure only up to 400m, at that distance we still observed some communication, providing indication that the range can be slightly larger. In the following Chapter 4, we will present the model validation using both of these path loss models and compare the model's overall performance using each of both as input for the L_{free_space} component.

3.6 Experiments Conclusion

All of these experiments provided us with the data needed to feed our model to estimate RSSI values and compare them furthermore with RSSI values of scenarios described in the following chapter. More extensively, we can conclude that:

- In consequence of the experiment described in Section 3.2, we could narrow down the installation points on the bicycle to the positions that we consider more attractive;
- Following with the experiment of Section 3.3, we have not only build our L_B component of the model, we have also learned that the human body can attenuate signal up to 15 dB;
- Similar to the previous point, we have captured radiation patterns around the car for Section 3.4, using the PE setup and our DME setup, assembling data for L_C and learn overall effectiveness of each setup wireless link quality;
- Experiment 3.5 provided us with the L_{free_space} data while also exhibiting the range of the DME bare antennas without obstructions.

Chapter 4

Evaluation of B2X Propagation Model

In this chapter, we evaluate the quality of our propagation model for bicycle-to-vehicle scenarios. In previous experiments we have collected the data to characterize the impact of the bicycle-cyclist body and the car's structure in the wireless communication as well the losses through the free space path loss. We include those elements in our propagation model, and evaluate the accuracy of the RSS estimates in representative Bicycle-to-Car scenarios against real-world data.

In the first section (Section 4.1), the bike-to-car (B2C) model is presented and our contribution is highlighted. Section 4.2, we present the scenarios we chose to simulate and challenge our model, and how the procedure to collect its data. Section 4.3 describes the experimental procedure we went through to simulate such scenarios. Then, in Section 4.4, we go through every scenario and observe the results.

It is important to remark that the contents of Section 4.2 and Section 4.3 are common to Chapters 4 (Propagation Modelling) and Chapter 5 (Data-Link Characterization).

4.1 The B2C model

The model we propose in this thesis gives a rough estimate of RSSI of a WiFi link between two vehicles, namely a bicycle and a car, given their positions with no obstructions between them (i.e. other vehicles, infrastructures).

Our contribution is to add two more elements to the Eq. 2.1, which are the losses through the bicycle and car's bodies. We add our contribution of vehicles frames with L_B and L_C :

$$P_{RX} = P_{TX} + L_{free_space}(d) + L_B(\gamma) + L_C(\gamma) + X_\sigma \quad (4.1)$$

- P_{rx} = Expected power to given positions of both nodes
- P_{tx} = Base transmission power of the transmitting antenna
- $L_{free_space}(d)$ = is the path loss which, as previously mentioned, is the input of attenuation caused by propagation for the distance d

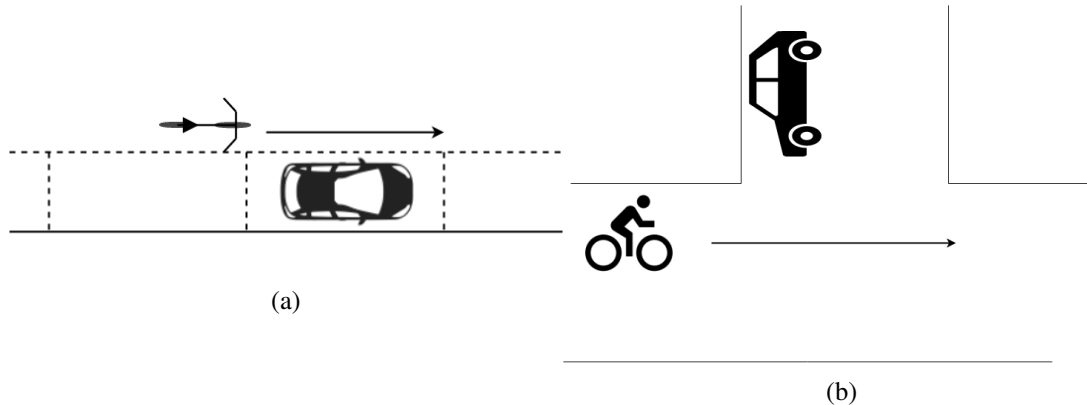


Figure 4.1: Selected representative scenarios: (a) parallel movement of bicycle overtaking parked car; (b) perpendicular movement in crossing roads with LoS;

- $L_B(\gamma), L_C(\gamma)$ = attenuation caused by (B)icycle-cyclist shadowing and (C)ar's shadowing in function of angle γ
- X_σ = slow fading (not considered / modelled)

With the Log-Distance Path Model [9], we can estimate the path loss through an empirical model, i.e., through field measurements (as we have covered in Section 3.5). Another model for path loss we consider is the Two-Ray Ground Reflection model. This model takes into account, that for a link with LoS, the losses through direct link and the interference of the signal that reflects on the ground, given the height of both transmitting antennas and the distance between the two. A comparison between these two path loss models was made in Section 3.5 and can make up L_{free_space} . We will try and use them both for our model.

We have composed a set of data from the experiments in Chapter 3, which the radiation patterns fit for the L_B and L_C components, so we get the attenuation for a given angle and the L_{free_space} with the previously mentioned models, which are functions of the distance between the vehicles. X_σ is a variability factor which induces the volatility of the signal, but for the validation of our model we have not implemented it and is opened up for future work.

4.2 Validation Scenarios

In order to validate our model, we have staged two scenarios in an urban environment that we believe to be representative of common interactions between bicycles and other vehicles. The selected scenarios were as follows:

- Bike approaching car's behind (Fig. 4.1a): this scenario was chosen for a perspective of a application of warning any driver that has parked its car of approaching cyclist and to be cautious of getting out of the car and hitting the cyclist with the door; and also can mimic when a bike and a car share the same lane.

- LOS bike-car crossing (Fig. 4.1b): the idea behind this scenario is just to characterize a simple cross of a bicycle and car, which link performance is important for such critical situations and can help prevent collisions.

A third scenario with obstructions was an option and we have collected data, but later realised it does not match with the expectations of our RSSI predicting model. Further details of such scenario can be found in the appendix.

4.3 Experimental methodology

We have used the same location as previous experiment described in Section 3.4 in a parking lot in Leça de Palmeira (see Fig. 3.6a) for the interactions without any obstructions, where the bicycle was ridden in a straight line of 400 meters back and forth with the car in the middle. Considering we wanted to evaluate both WiFi off-the-shelf products and built-in WiFi hotspots of cars, the following setups were used to achieve our results:

- **Dedicated Measurement Equipment (DME):** This setup consisted of only using the same antennas to simulate a car's WiFi setup and evaluate its performance for infotainment and efficiency applications (e.g. audio streaming). We evaluate **continuous data transfer** using active network measurement tool iPerf [23], transmitting UDP datagrams from the bicycle (client) to the vehicle (server) with a default transmit power of 20 dBm. These datagrams had a 1470 Bytes size and a offered load of 56 Mbps. The data rate is automatically adjusted by the antenna module in the range of 1 to 54 Mbps using a proprietary algorithm. This setup consisted of: a laptop connected to a GPS tracker placed on car's roof and two antennas next to the rear-view mirror (see Fig. 4.2) one configured into ad-hoc mode and the other one to monitor mode; the bicycle used the same equipment as PE, using a laptop connected to an antenna configured in ad-hoc mode and a GPS tracker. Then a script would be run that make a iPerf connection and save its output, record the packets through tcpdump and keep the track of GPS positions (1 position per second).
- **Production WiFi Equipment (PE):** This setup was used to capture the RSSI of **periodic beacons** from the car's AP, with a default transmitting power of 18 dBm and a beaconing rate of 1 Mbps for 214 Bytes sized packets. It consisted of: a laptop inside the vehicle while the GPS tracker was placed on the roof to keep the car's position; another laptop was held to the bicycles rack connect to an antenna, configured in monitor mode, and GPS tracker in the middle-point of the handle bar. Both PCs would run a script that would save the RSSI samples of the beacons through tcpdump and record GPS positions (1 position per second).

In this Chapter we evaluate the B2C model against data of the DME setup only.

The car was parked in place and the bicycle would be ridden for three iterations of laps (3 times back and forth) after running the scripts, riding as slow as possible while the whole system



Figure 4.2: Experimental setup used in DME and PE setup with GPS tracker and antennas on the car’s rear-view mirror

was operating and collecting data. When finished, we would switch setups and restart scanning, and then repeat for the remaining scenario.

In summary, this was the sequence of the sampling process:

1. Choose scenario and position both vehicles
2. Configure and prepare desired setup (either PE or DME)
3. Run measuring scripts and do 3 laps of riding the bicycle (back and forth)
4. Once all laps were done, stop the script and verify the samples were correctly recorded

This sequence would be repeated for each session of the experiment.

4.4 Results

In this section we describe the data processing of the RSSI values we have captured throughout all experiments. This is done by a comparison of our B2C model, through information gathered in previous experiments (described in Chapter 3), to the samples captured in the scenarios (as mentioned in Section 4.3). To explore this, we tackled every element (but slow fading) in the equation Eq. 4.1.

The model validation was only made with the values recorded through our DME setup. Once every constant is defined (e.g. Log Distance’s α , Two-Ray antennas heights), our input variables d and γ are calculated within the scripts given the GPS coordinates. Components L_B and L_C return a relative attenuation of the signal in dBm given the angle of communication relative to the other node, as portrayed in the bicycle’s (see Fig. 3.5) and the car’s (see Fig. 3.8) radiation patterns and for this purpose we have created look up tables for easier access for such values. These look up tables consist of a attenuation given a angle, and for angles that do not make part of the

table an interpolation is done between the two nearest angles; this table therefore serves as a quick reference of attenuation of a transmitted signal for certain angle on the mounted vehicle. In Section 3.5, we conducted a experiment to obtain the values of the Log Distance Path Loss model (Pl_0 , α and d_0) through linear regression of the samples we have obtained these parameters for the linear function that forms L_{free_space} and only depend on the distance. The Two-Rays Ground Reflection model is another function that we will use for L_{free_space} and only variable is the distance between nodes, given that the antennas height remain constant.

Since we have marked each moment we collected a sample we can map out RSSI values to positions at each moment and compare it with what we were expecting in our model. In the following sections, the collection of RSSI samples are represented for each scenario we have selected (i.e. parallel, perpendicular) along side the prediction of RSSI of our model according to the vehicles conditions (distance and angle between them) using either Log Distance model (LD) or Two-Rays Ground Reflection model (TR) as the path loss components.

A quantitative evaluation of the model accuracy is provided by a set of histograms for each application that shows the relative number of differences between a RSSI value predicted by the B2C model and a RSSI sample captured during the experimental sessions. These differences represent the **estimation error** and indicate the offset from the captured sample that was predicted by our model in dBm.

4.4.1 Parallel scenario

The Figure 4.3 present two time series of the sampled RSSI values alongside: Figure 4.3a the prediction model using the Log Distance model (LD) for path loss, Figure 4.3b the prediction model using the Two-Rays Ground Reflection model (TR) for path loss; both with and with out the contributions of the bicycle-cyclist (LB) and car's (LC) bodies.

In those results we can observe a pattern of RSSI samples that we have sectioned as depicted for Fig. 4.3a. These sections represent 4 distinct arrangements that are repeated sequentially for the rest of the experiment. Acknowledging that in this scenario we start with the bicycle and car facing each other, and that the Fig. 4.4 depicts the contribution of the LB and LC components (bicycle and car respectively), we can analyse the values of the RSSI samples:

1. This is the start of the lap and this moment ends when it crosses the car. This setting has the bicycle and the car facing each other, which means the antenna is not blocked by the cyclist body and the antenna does not have to go through the car's back. We can notice that the values are disperse at the longer distance and when about to cross the car, while being consistent mid-way. This can be explained by the power that is attenuated inconstantly for each packet at long distances and reflections on the car's structure at smaller distances.
2. After crossing the car, the cyclist and the car have their back turned to each other. This setting is the most severe in attenuation due to both the cyclist body and the car's body and interior elements (remember that the DME is positioned at the front of the car) being

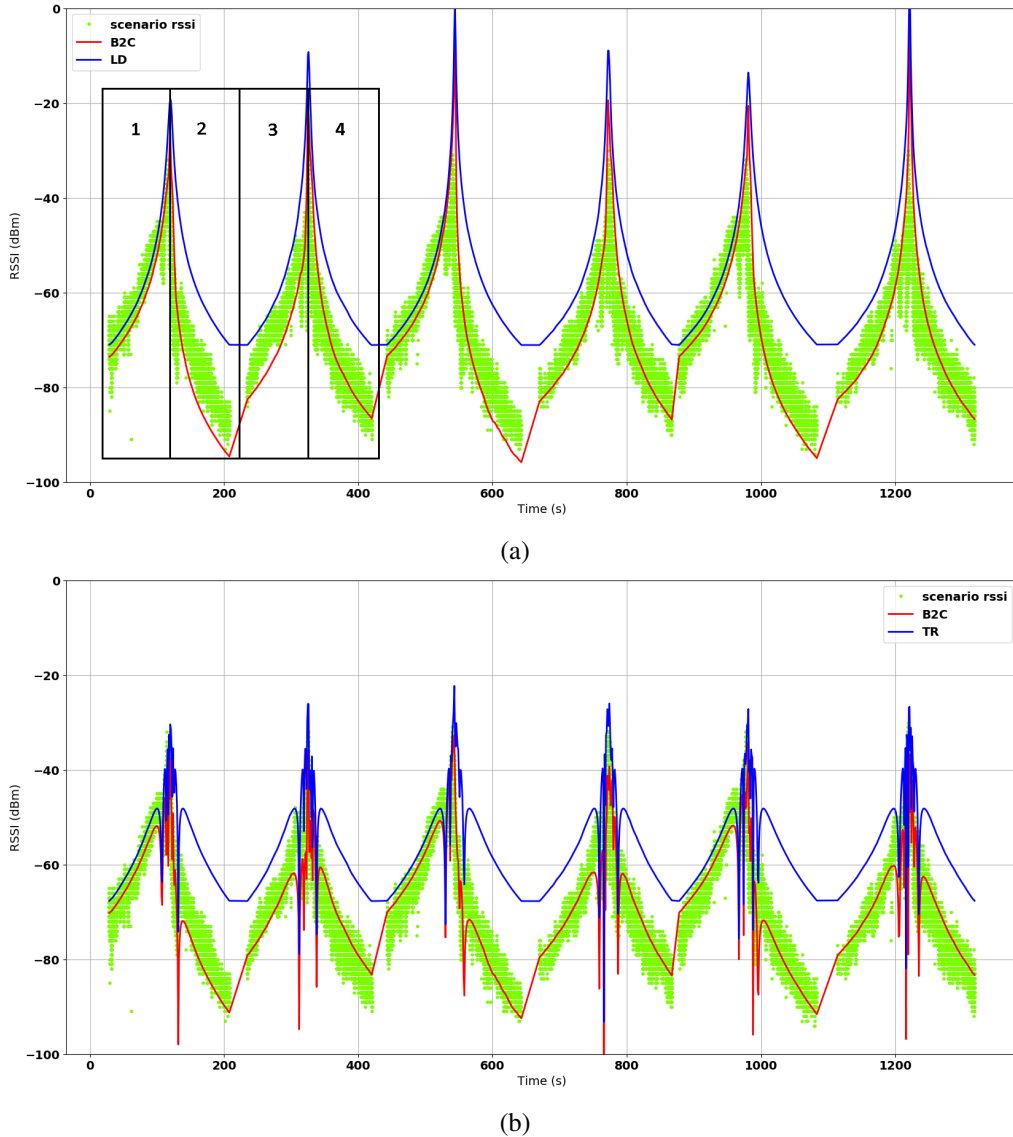


Figure 4.3: RSSI Samples (green dots) from the **parallel scene**, overlaid with RSSI model prediction using either (a) Log Distance model or (b) Two-Rays model as the path loss component and comparison of the introduction of influence of bicycle-cyclist and car's bodies (red line) to their absence (blue line).

in-between the communicating antennas, hence originating a wider range of RSSI samples and lower values.

3. The bicycle turns around and now the cyclist is facing the back of the car. The main obstruction is the back of the car, and the values are only slightly lower than at situation 1. The moment the bike crosses the car we can notice a bigger dispersion in values.
4. On the way back to the start, the cyclist's back is facing the car's front. The cyclist's body is between the communicating antennas which causes the RSSI values to drop, but not as steeply as we can observe in the situation 2 because the DME is at the front of the car. When

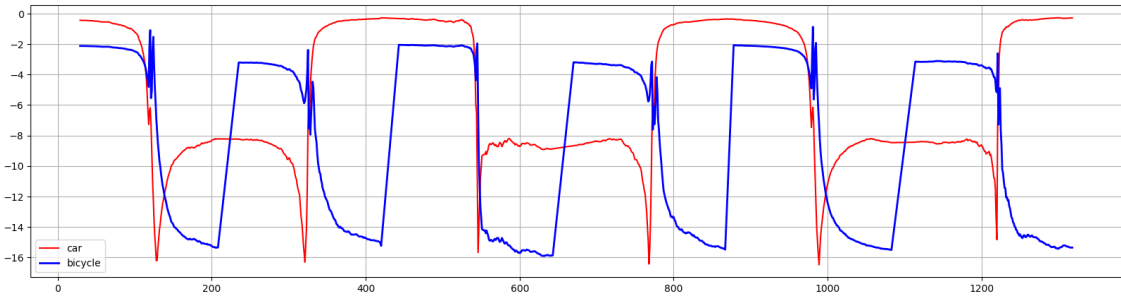


Figure 4.4: RSSI attenuation contributed by cyclist-bike (blue) and car (red) bodies in the B2C model for the **parallel scenario**.

the bicycle reaches its end, it turns around to start another lap, and we can see a increase in the RSSI values.

After describing the movement patterns and observed RSSI behaviours, we want to also comment the RSSI indicated by the B2C model:

- **Figure 4.3a:** The model, when applies the LD path loss model, correctly follows the trend of RSSI values. We can see that when the bicycle is the nearest to the car it tends to overestimate and we can see that it reaches positive values of RSSI, which is not feasible and realistic - it happens due to the fact for short distances our empiric Log-distance model provides higher values as seen in Fig. 3.10. In situations 2 and 3 we can observe a underestimation, which can mean that the model estimates the car's back to attenuate more than it should, about 10 dB off the mean value. Nonetheless we can notice that it is consistent in its behavior according to the RSSI samples and it can be accurate for periods that the distance correspond to RSSI values in the range between -70 and -50 dBm;
- **Figure 4.3b:** When the TR path loss is applied, we can observe it following the RSSI estimation trend. It predicts the big rise followed by a dip right before getting near the car. The RSSI prediction using TR present many dips as the bicycle approaches the car. The dips are predicted by the TR model with the contribution of a reflected ray from the ground, which interferes destructively with the direct ray at short distances between wireless nodes. In our measurements we observe some of those dips, but we can not identify clearly those that happen nearer the car.

The three error histograms (see Fig. 4.5) allow us to evaluate quantitatively the accuracy of the B2C model using the errors, which consist of subtracting every captured RSSI sample to the predicted value by the value that the model has indicated at that moment. Therefore, negative values represent an underestimation and positive values an overestimation of the real values.

- **Histogram 4.5a and Histogram 4.5b:** Both histograms depict the B2C model using either path loss model (i.e. TR and LD) against their free space counterpart. It is depicted in the Fig. 4.5a that when we consider the bodies of the cyclist-bicycle and the car, 65% of the

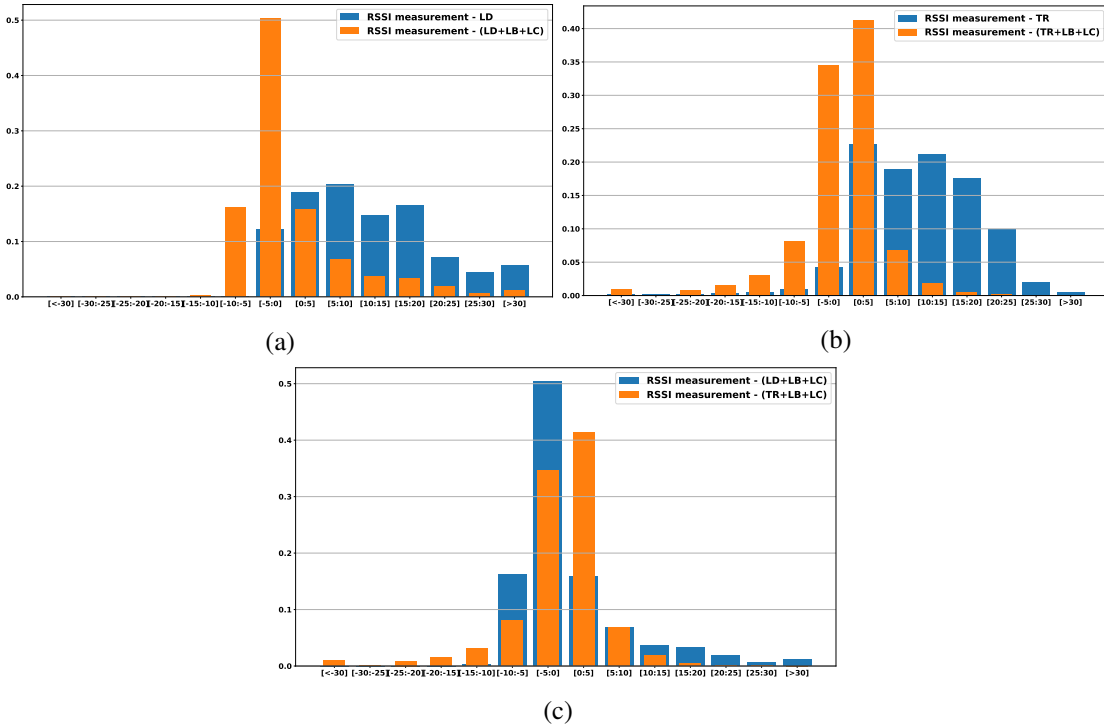


Figure 4.5: Histograms for performance of the B2C model for the **parallel scene**, using (a) Log Distance, (b) Two-Ray Ground Reflection as path models, and (c) comparing each other's performances

predictions are -5 to 5 dBm near the actual value, versus when we do not actually consider the bodies of 30% of the values. Additionally, 85% of the values are in the error range of -10 to 10 dBm, the LD model itself still overestimates most the values, having 50% of the values in that range, and overestimating by at least 5 dBm, around 65% of the values. When we consider the bodies using the TR path loss model, we can observe from the Fig 4.5b: 75% of the values that the body attenuation was included they fall in the -5 to 5 dBm error range, compared to about 28% of free space that fall in that same range; we can also see that about 63% of the values from the not inclusion of L_B and L_C are more than 5 dBm off the real value.

- **Histogram 4.5c:** This histogram compares between the contribution of path loss models in the prediction model. We can observe that the use of TR has more values (75 %) in the range of -5 and 5 dBm than RRSSI estimates using LD (65%). We can also observe that the TR path loss model covers more bins than the LD, which we can also mention how centralized in the bin [-5:0] the B2C model using LD is, indicating that it mostly underestimates the values down to -5 dBm.

From these analyses we can observe that:

- The inclusion of the attenuation caused by the cyclist-bicycle and the car it is shown to have more precision than only considering free-space and use solely the path loss models.

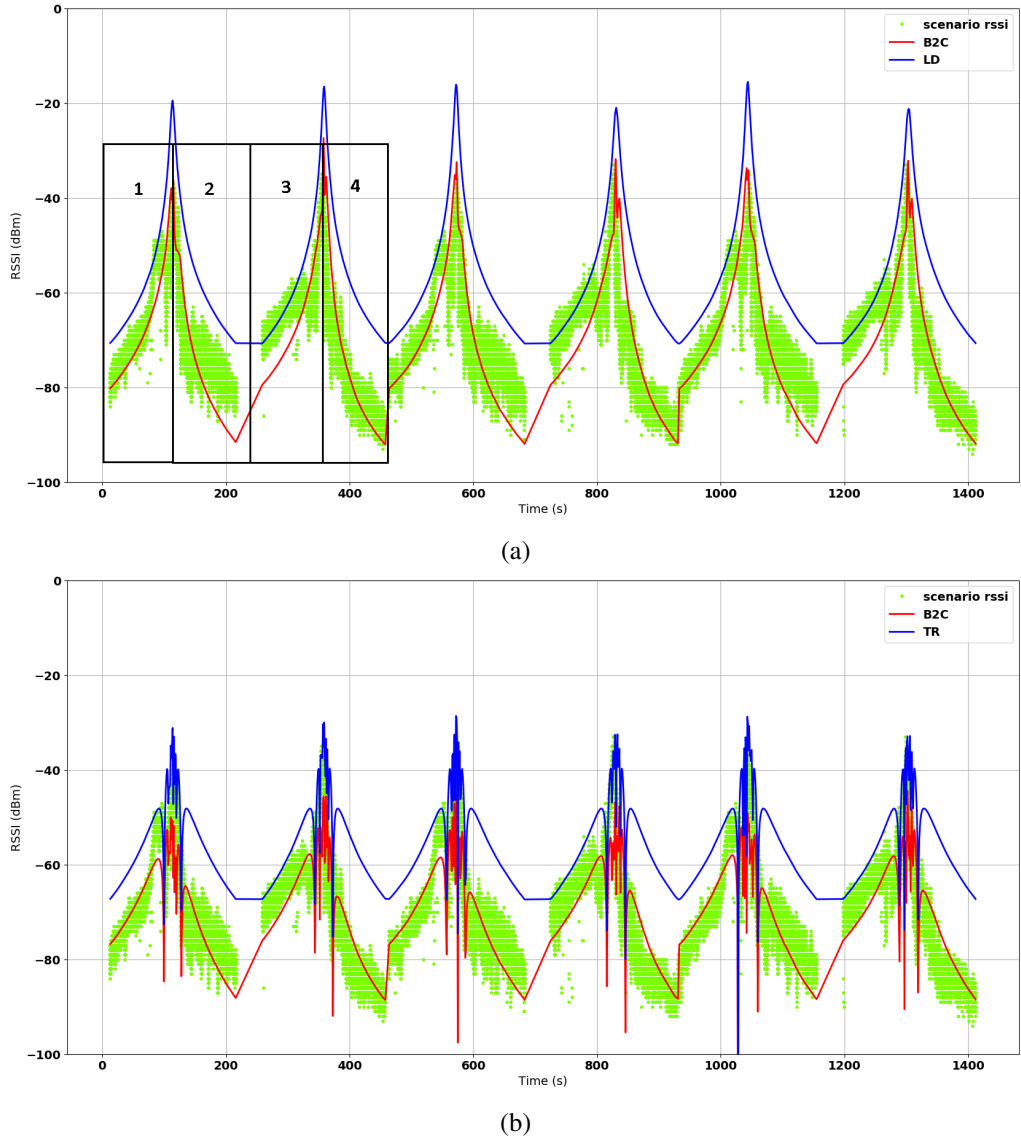


Figure 4.6: RSSI Samples (green dots) from the **perpendicular scene**, overlaid with RSSI model prediction using either (a) Log Distance (B2C is orange, LD is blue), (b) Two-Ray Ground Reflection as path models (B2C is orange, TR is blue), and (c) comparing each other's performances (TR is orange, LD is blue).

- The usage of TR seems to have a better precision than LD, although it has a greater variability in its values.

4.4.2 Perpendicular scenario

The Figure 4.6 present two time series of the sampled RSSI values along side: Figure 4.6a the prediction model using the Log Distance model (LD) for path loss, Figure 4.6b the prediction model using the Two-Rays Ground Reflection model (TR) for path loss; both with and without the contributions of the bicycle-cyclist (LB) and car's (LC) bodies.

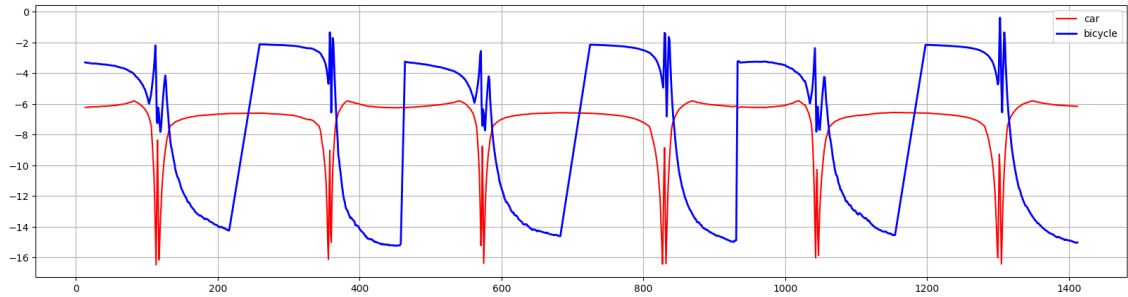


Figure 4.7: RSSI attenuation contributed by cyclist-bike (blue) and car (red) bodies in the B2C model for the **perpendicular scenario**.

In these results we can observe a pattern of RSSI samples that we have sectioned as depicted for Fig. 4.6a. These sections represent 4 distinct arrangements that are repeated sequentially for the rest of the experiment. Acknowledging that in this scenario we start with the bicycle facing the car's front left side, and that the Fig. 4.7 depicts the contribution of the LB and L_C components (bicycle and car respectively), we analyse the values of the RSSI samples:

1. This is the start of the lap and this situation ends when it crosses the car's front. This setting has the bicycle facing the car's left side, which means the antenna is not blocked by the cyclist body but the car's metallic pillar will block the signal at some angles. We can notice a steep rise of the RSSI values with a noticeable drop and increase in variability when about to cross the car.
2. After crossing the car, the cyclist's back has the car's right side facing it. This setting has the cyclist body in-between the communicating antennas; this obstruction is more pronounced at longer distances where we can see a wider range of samples. We argue that the samples do not behave the same for a similar situation, like situation 4, due to the placement of the monitor antenna that can provide different LoS conditions - see Fig. 4.2. The bicycle turns around then, the gap to the next situation happens because we have only presented the samples up to a distance of 200 meters.
3. and 4, are similar to situations 1 and 2 respectively. In 3, the cyclist is facing the right side of the car. Then, from the crossing point to the end of the lap, the cyclist's back is facing the car's left side. In this situation 4 the cyclist's body is between the communicating antennas once again.

In the awareness of these patterns and cyclist movement , we want to also comment the RSSI indicated by the B2C model:

- **Figure 4.6a:** From this plot we can observe that the model prediction is very consistent in its behavior for each passage. The prediction underestimates at longer distances for situations like 2 and 3 (more pronounce in the first lap). We can note that the LD model does not consider ray reflections, so it does not present the dips that we can observe in the captured samples.

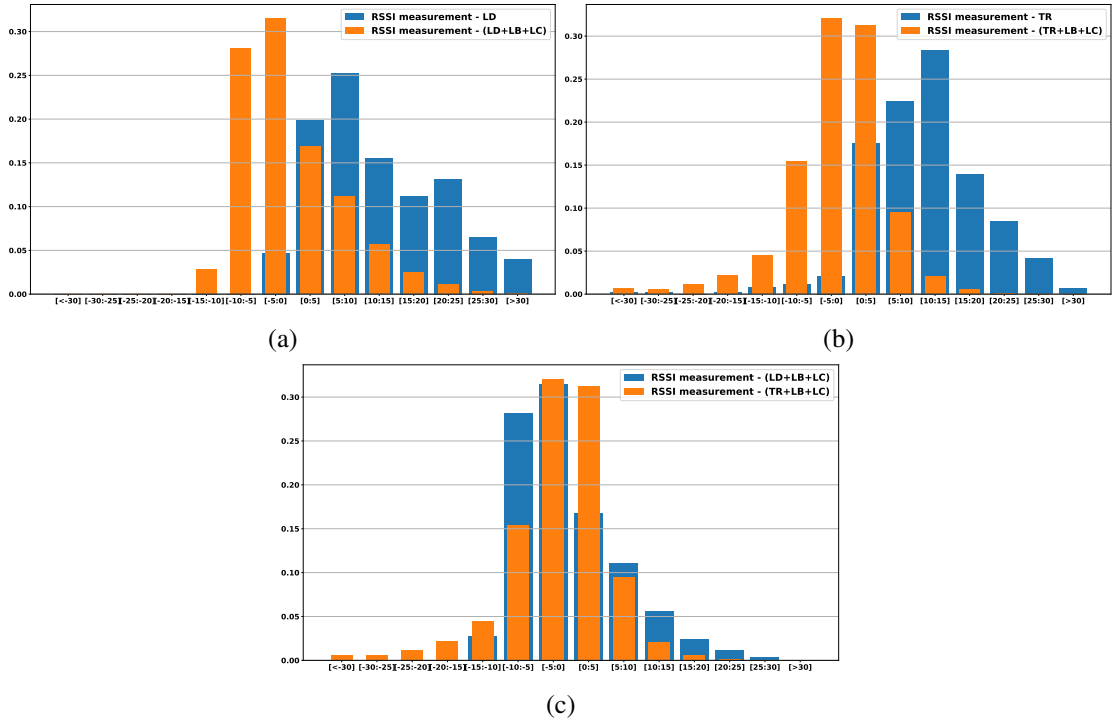


Figure 4.8: Histograms for performance of the B2C model for the **perpendicular scene**, using (a) Log Distance (B2C is orange, LD is blue) , (b) Two-Ray Ground Reflection as path models (B2C is orange, TR is blue), and (c) comparing each other's performances (TR is orange, LD is blue)

- **Figure 4.6b:** The usage of TR as the path loss model, apart from some sporadic underestimated dips in distances nearer the car, it mimics very much accordingly with the samples.

To further support the analyses, we have plotted three error histograms (see Fig. 4.8).

- **Histogram 4.8a and Histogram 4.8b:** It is shown clearly that the consideration of the attenuation of the bodies (L_B and L_C) greatly improves, to when compared to solely using the path loss models. The usage of LD has 47 % of its values in the range of -5 dBms to 5 dBms, while using only the free space has 25%. Since most of the values of the free space are overestimated, we can see that 75 % of them are at least 5 dBm away from captured values. This Histogram 4.8b also depicts a great improvement through the consideration of shadowing caused by the cyclist-bicycle and car. Having 63% of its values in the range of -5 dBm to 5 dBm and about 20% by the free space model. When we only considerate the free space (i.e. absence of obstructions) 77% of its values are at least 5 dBm over the sampled values.
- **Histogram 4.8c:** This histogram shows the performance of the usage of TR compared to the LD usage. Using the TR path loss model has resulted in 63% of the predicted values to fall in the range of -5 dBms to 5 dBms from the real values, while for the LD model this value is only 47%. Meanwhile, in the range of -10 dBms to 10 dBms, the LD usage has

85 % of the values and the TR usage 87 %. The TR contribution seems to provide more accurate estimates.

Through these analyses we have learned that:

- The inclusion of the attenuation caused by the cyclist-bicycle and the car it is shown to have greatly improved the precision than only considering free-space and use solely the path loss models.
- The usage of TR seems to have a better precision than LD, and it has modelled some dips observed in the captured values that the LD usage does not.
- Comparing to the parallel scenario, the usage of TR is more precise to using LD as the path loss component in both scenarios.
- On the other hand, the captured RSSI samples from the parallel scenario were less disperse than this crossing scenario, which means this scenario is more prone to signal degradation.

4.5 Conclusion

We began with joining the attenuation induced to the signal (by the bodies of bicycle-cyclist compound and the car's frame) to two existing path loss models (Log Distance path loss model and Two-Rays Ground Reflection path loss model). We have gone through extensive experiments in order to characterize the radiation patterns of WiFi antennas placed on the bicycle with a rider and a car and then use them for the components contained in our RSSI predicting model, $L_{free_space}(d)$ for path loss, $L_B(\gamma)$ for attenuation caused by the bicycle and cyclist and $L_C(\gamma)$ for the shadowing caused by the car's body. Then we have staged a set of representative scenarios (i.e. parallel and perpendicular with LoS) and recorded RSSI values to compare to our model in the same conditions. We conclude that our model has more precision than solely using a path loss model for all the scenes we have sampled, although is only reliable for scenarios without obstructions between the two nodes. We have also gathered that for LoS scenarios, the TR model is generally a better addition to our model than the LD. The results have shown that the B2C model has increased reliability to path loss models while it also is open for improvement of each component as future work.

Chapter 5

Opportunistic Use of In-Vehicle Wireless Networks for VRU Interaction

The text of this chapter is adapted from an article [24] and dedicated to a by-product from our car's WiFi measurements and it is about vulnerable road users (VRUs), such as pedestrians, bicycles and motorbikes, make use of a car's built-in WiFi hotspot for their protection and/or infotainment. For such, we have evaluated the quality of the link through the measurements made in the representative scenarios with the throughput and RSSI of each packet of our setup and IRT and RSSI of each beacon of the car's AP. The scenarios and experimental setup used in this chapter are those described in Chapter 4. We want to observe how this link can enable a variety of applications for VRUs while also learn about its limitations.

5.1 Experimental Evaluation and Results

The measurements which made up the data for this chapter are the same used in the previous Chapter 4, as described in it.

From the extracted samples we have looked into three metrics:

- **Received Signal Strength Indicator (RSSI):** indicates the power level of received packets. This metric describes the link quality between transmitter and receiver nodes, which is affected by moving or static obstacles, system configurations, among other factors.
- **Throughput:** the maximum rate at which the wireless channel capacity is used for data transmission, i.e. the successful message delivery rate over the wireless channel. This metric is specially relevant for infotainment (e.g. multimedia) or efficiency applications.
- **Packet Inter-Reception Time (IRT):** the time interval between consecutive successfully received packets. This metric is specially important for safety critical applications enabled by periodic beaconing.

Fig. 5.1 depicts the RSSI empirical distribution function for the parallel and perpendicular scenarios using the car's and our setup. For the parallel scenario, the results show that the RSSI

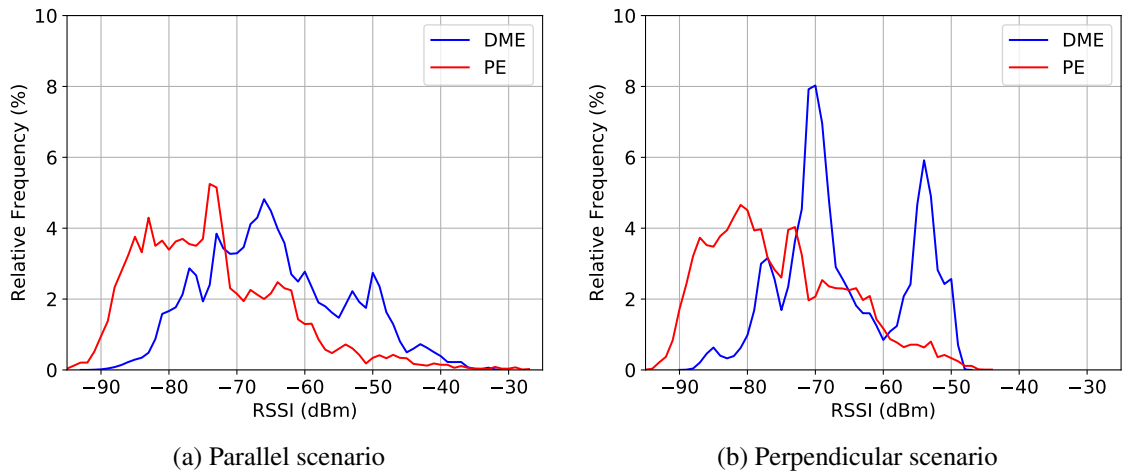


Figure 5.1: Received Signal Strength Indicator (RSSI) Empirical Distribution Function for two scenarios using PE and DME.

distributions are similar but offset by approximately 12 dB. We argue that this difference is due to the lower transmission power, larger cable losses and the less favorable antenna position of the PE system for communication to outside of the vehicle, which leads to fewer LoS conditions due to obstacle obstruction and bicycle mobility. Similar results are obtained for the perpendicular scenario.

Fig. 5.2 shows the RSSI as a function of distance for vehicle-to-bike communication. As expected, the RSSI decreases exponentially as the distance between communicating nodes increases. Additionally, we observe that the variations of the RSSI metric increase as the node separation increases due to the more pronounced small-scale fading. Analyzing a given scenario and setup (e.g. Fig 5.2a), we observe that human body shadowing causes the received signal power to decrease by approximately 10-19 dB due to the loss of LoS conditions for a wide range of angles between transmitter and receiver nodes; these results are larger than the ones reported in paper [14] that considered static conditions. The absence of the symmetry between both sides of the curves might be attributed to irregularities in the radiation pattern or asymmetries in the vehicle's structure as also reported in [25]; for the DME setup this effect also occurs due to the slightly shifted antenna installation with regard to the vehicle's transversal center.

For a given setup, we observe a larger decay and signal variability of the RSSI metric for the parallel scenario most likely due to additional obstructions between nodes created by the vehicle's structure. On the other hand, in both scenarios, the RSSI metric is lower for the PE setup when comparing with the DME setup due to the different configurations detailed previously. This is specially evident for the approaches/departures from the front (parallel scenario) / right (perpendicular scenario) of the vehicle that might be attributed to an antenna installation closer to the vehicle's center of mass.

Fig. 5.3 depicts the Throughput metric as a function of distance using the DME setup; results are not available for the PE setup because it was not possible to inject traffic without interfering with the experiments. The results show that - in both the parallel and the perpendicular scenar-

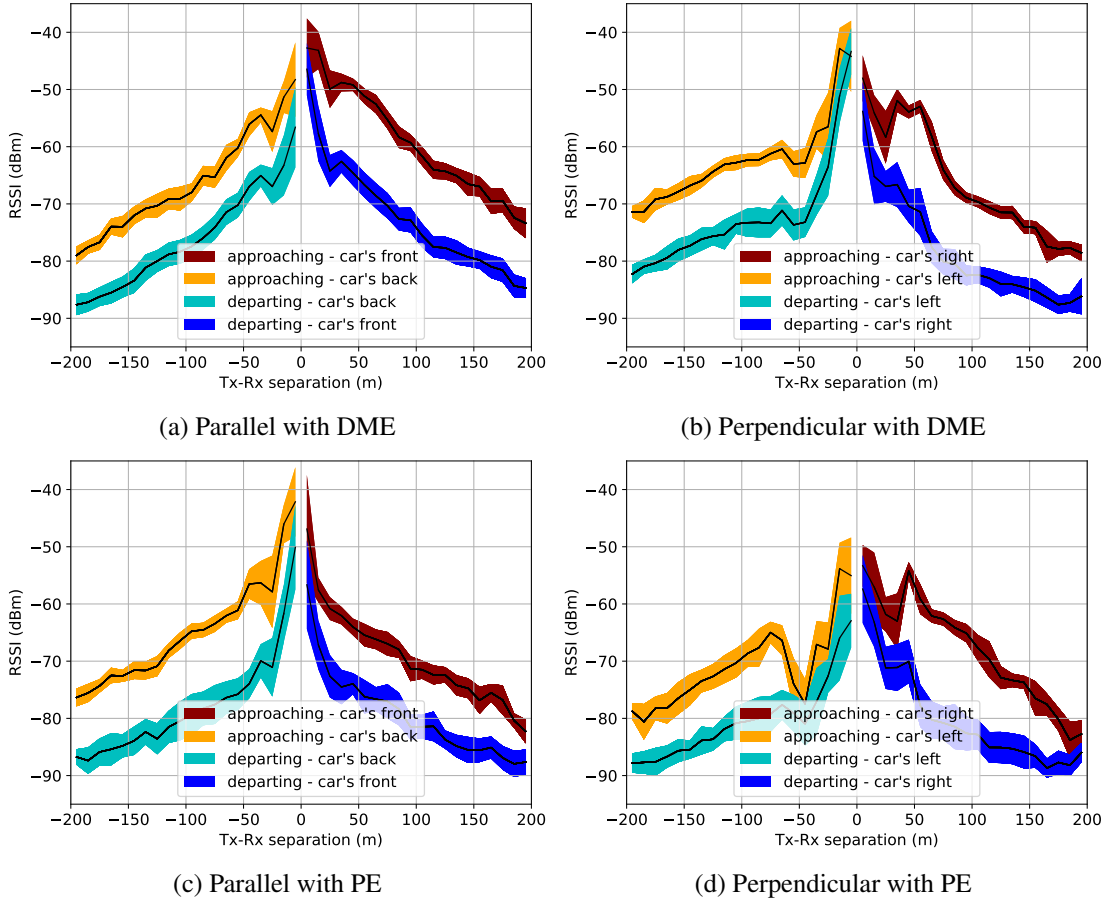


Figure 5.2: Received Signal Strength Indicator (RSSI). For each 10 m distance bin, we represent the mean RSSI and the corresponding one standard deviation around the mean.

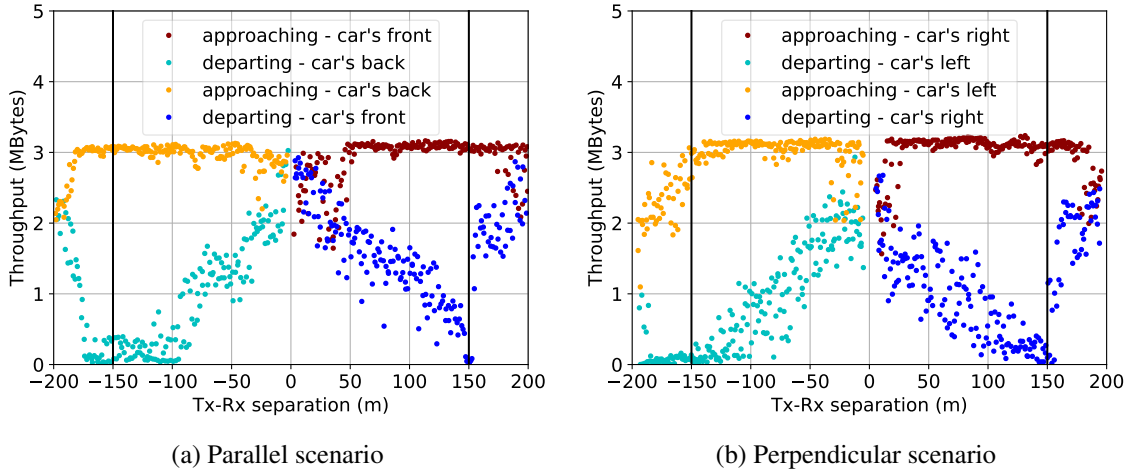


Figure 5.3: Throughput as a function of distance for DME. Each point corresponds to the average throughput per 1 s interval.

ios - nodes can successfully exchange large amounts of data up to at least around 175 meters for experiments without human body shadowing. On the other hand, experiments with reduced effective received signal power (e.g. due to human body shadowing) suffer from a sharp decrease

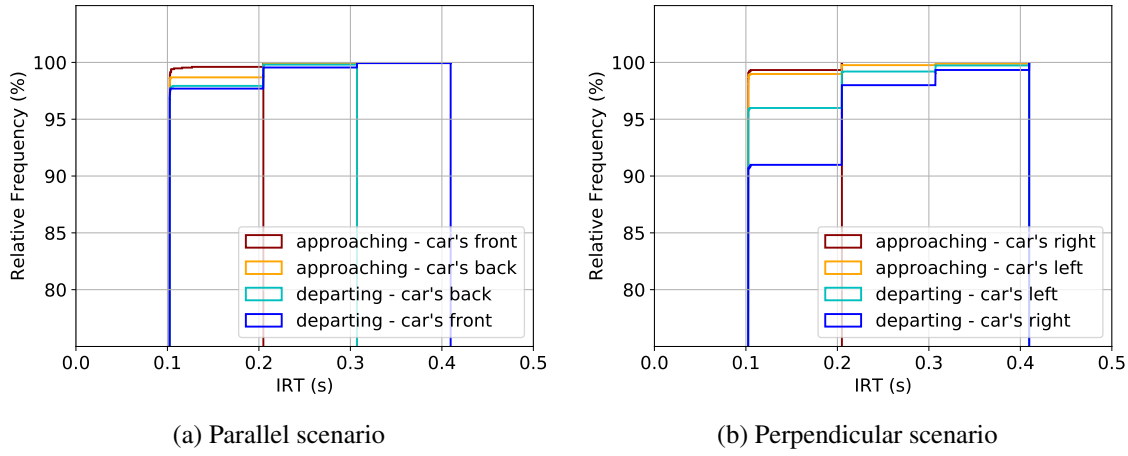


Figure 5.4: Packet Inter-reception Time (IRT) CDF for Parallel and Perpendicular scenarios using Production Equipment (PE).

of the throughput as the node distance increases given the more aggressive rate adaptation. The more challenging propagation conditions reduce the maximum communication range for infotainment applications to bellow 100-150 meters, and an even smaller effective communication range depending on the application requirements.

Fig. 5.4 depicts the packet Inter-Reception Time (IRT) Cumulative Distribution Function (CDF) for the Parallel and the Perpendicular scenarios using the PE setup. We observe that the vast majority of the time (100% and 98.3% for the parallel and perpendicular scenarios, respectively) the IRT is below 400 ms. The results show that the probability of burst errors is low, which suggests that the system is able to support safety applications with stringent time requirements given the low probability of awareness blackouts (i.e. high IRT values), specially in the parallel scenario and for LoS conditions (i.e. approaching situations without human shadowing).

5.2 Conclusion

Our empirical results show that an opportunistic ad-hoc communication system is able to support a variety of safety (e.g., collision warning), efficiency (e.g. data offloading) and infotainment applications, specially in the most relevant scenario where the bicycle approaches a car (i.e., the IRT is below 400 ms and the throughput is around 3 MBytes). We also observed that human and vehicle structure shadowing and the scenario type affect the link quality and the system performance in terms of IRT, which indicates that different communication configurations may be necessary depending on the spatial arrangement of vehicle and VRU. The performance obtained using the OEM's production equipment can be improved with a more favorable positioning of the antenna for communication to outside of the vehicle.

Chapter 6

Conclusion

6.1 Final thoughts

To conclude, with this thesis we have went through various experimental steps to strengthen our model. We have tried to define antenna positions to fit our criteria and carry other experiments. We have made conducted experiences to feed values to our model, such as approximate radiation patterns for ridden bicycles and cars and performance of bare antennas. Lastly, we simulated a set of representative scenarios to evaluate and compare to our model precision. We have also make use of the car's hotspot and evaluated how feasible it is for VRUs use and compared it to our own dedicated setup. Our contributions consist in:

- Radiation patterns for various mounting points of the WiFi antenna on a bicycle with out a rider;
- Radiation pattern for three different antenna positions with rider included;
- A car's radiation characterization using a off-the-shelf antenna and its own built-in WiFi antenna;
- Characterization of WiFi communications from a set of representative scenarios using WiFi antennas mounted to a bicycle and a car;
- Analyzes of opportunist use of a car's WiFi system for security and/or infotainment applications;
- A RSSI predicting model that considers attenuation caused by cyclist-bicycle and the car's bodies.

This thesis has become a great learning experience. Not only we have learned at a greater depth the behavior of the WiFi (IEEE 802.11b/g) technology, some effort went also into designing, preparing the experiences and hands-on work. Throughout the work, we have learned and improved the measurement tools from the previous experiment and kept sharpening our perception and understatement around our objective. Each experiment had its own written guide on how

to carry them, its own unpredictable errors and technical difficulties, its own measuring scripts and updated ways of representing the results.

6.2 Future work

The model we have designed it is capable of giving a rough prediction of WiFi's RSSI performance for a given position of two communicating vehicles but there is a big room for improvement. Its modular design allows to work on its unique terms of the equation:

- The constants build from the Log Distance Path Loss Empirical model is not as precise as we would wish. It was done in an urban environment and every 20 meters. The results could have been affected by noise interference and the measurements being done in a smaller step to increase precision, positive values are not representative of the reality.
- Our look up tables were built from our experiments of radiation patterns. These experiments can be further improved, given they were done in interference prone environment and not in an anechoic chamber. Additionally, the car's radiation pattern was done only to one of its side, since we have considered to be transversely symmetric.
- The locations chosen for RSSI sampling of the selected scenarios were interference prone.
- In the B2C model, the X_σ slow fading component was not evaluated and its addition is open for future work.
- Despite rigorously attempting to execute the experiments and trying to reduce external factors to influence its procedures and results, errors and a few imprecisions were condemned to happen.

Appendix A

Appendix

A.1 The B2C model in a non LoS scenario

The **NLoS bike-car crossing** (Fig. A.1) scenario mimics the real-world situation of a car and a bicycle meeting perpendicularly at an intersection, we wanted to characterize a scenario where there is no line of sight and is even more crucial when the cyclist and the driver are not aware of each other.

Our model does not consider obstructions (e.g. other road users, building's walls) and for such it is expected to have a over estimation of the RSSI values, i.e., that the model will indicate that the link will have a better performance than it actually does.

We went to a nearby block to make use of intersections (see Fig. A.2) for the NLoS scenario, where the distance of the bicycle path was 200 meters and the bicycle was ridden back and forth on a nearly straight line with the car at the middle point. We chose it because it had a leveled ground, nearly perpendicular with walls close to the road and low presence of other vehicles driving by and parked.

A.1.1 Results in a non LoS scenario

This scenario differentiates from others because it includes the presence of obstructing buildings, and the B2C only considers the attenuation caused by the cyclist-bicycle and car added to the free space path loss models (TR or LD). As such, we do not expect accurate estimates in this scenario; our goal is to obtain a rough quantification of the accuracy degradation of the model estimates in non-LoS conditions and in presence of other vehicles acting as obstacles. Nonetheless, we will make the same procedure in analysing the data, and evaluate the B2C model performance in such non LoS scenarios.

The Figure A.3 presents two time series of the sampled RSSI (yellow) values along side: Figure A.3a the prediction model using the Log Distance model (LD) for path loss, Figure A.3b the prediction model using the Two-Rays Ground Reflection model (TR) for path loss; both with (red) and with out (blue) the contributions of the bicycle-cyclist (LB) and car's (LC) bodies.

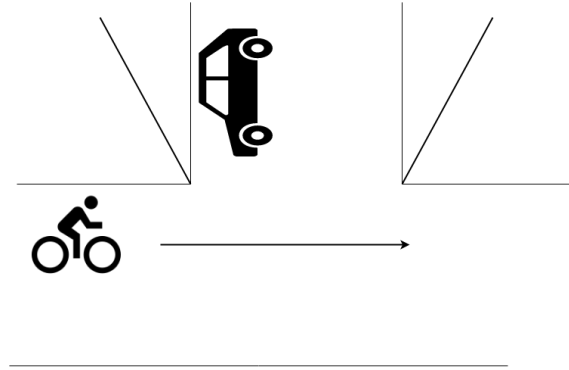


Figure A.1: Depiction of NLoS scenario

In these results we can observe a pattern of RSSI samples that we have sectioned as depicted by Fig. A.3a. These sections represent 4 distinct arrangements that are repeated sequentially for the rest of the experiment. For this scene we can observe the cuts being made in time, this happened due to its imbalance in distances ridden at the samples were capped to 96 meters from the car so it was the time it took to turn around. Acknowledging that in this scenario we start with the bicycle facing the car's front left side, we analyse the values of the RSSI samples:

1. This is the start of the lap and this moment ends when it crosses the car's front. This setting has the bicycle facing the car's left side, but given we have buildings obstructing, the RSSI sample ranges are very wide. When the bicycle gets closer to the car the RSSI samples rise due to being in LoS with the car in the middle of the intersection.
2. After crossing the car, the cyclist's back has the car's right side facing it. This setting has the cyclist body in between the communicating antennas, this is observed in a greater depression of the values.
3. In this situation, the cyclist is facing the car's left and we can notice the rise of the RSSI values due to no human body obstruction, yet having infrastructure blocking the signal strength.
4. From the crossing point to the end of the lap, the cyclist's back is facing the car's left side. The cyclist's body is between the communicating antennas one more time, like situation 2. We can notice even higher spread of the values, which have been caused by the building walls. The interference might be different because these might contain different objects that interfere the signal differently.

In the awareness of these patterns and cyclist movement , we want to also comment the RSSI indicated by the B2C model:

- **Figure A.3a:** Our model seems to follow the RSSI values trend well when the bicycle is afar from the car, but not in closer distances. We can also see that our prediction is generally higher than the captured value because we do not considerate the attenuation caused by infrastructures.

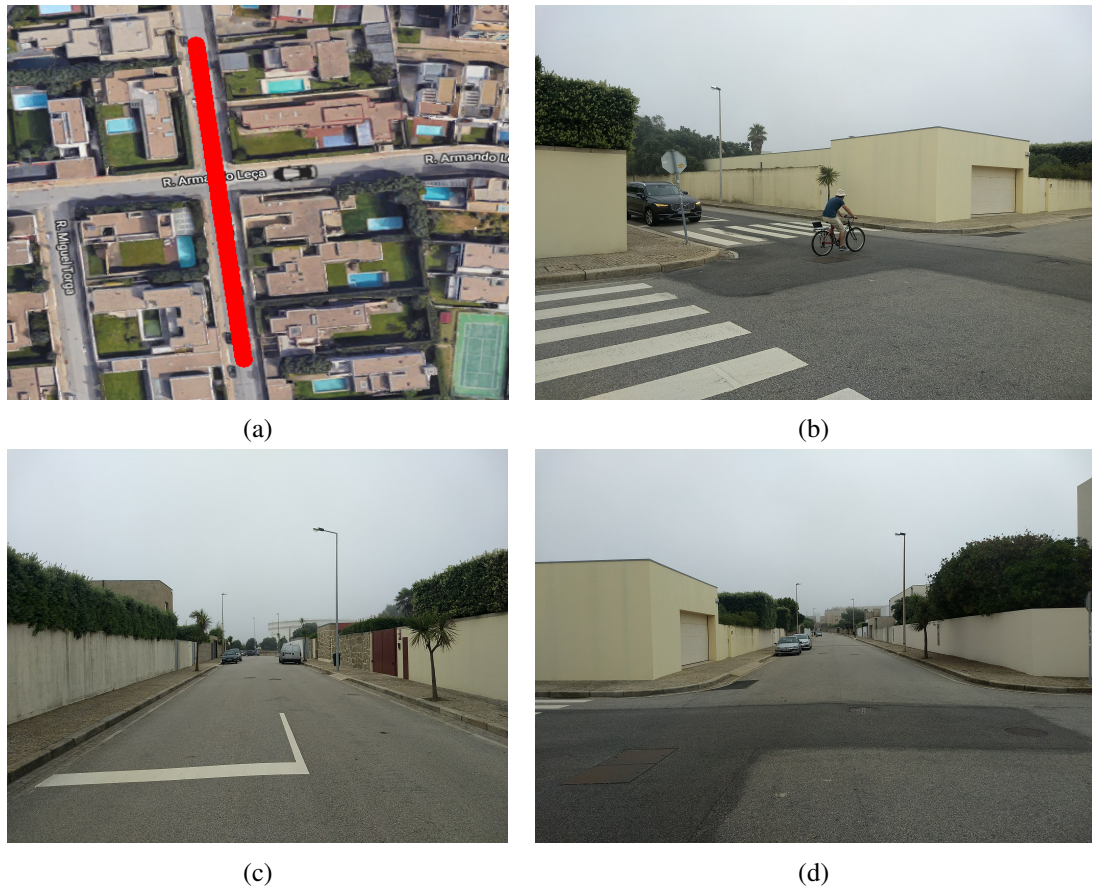


Figure A.2: Location and bike's path used to capture RSSI samples for a scenario with no Line-of-Sight. Figure (c) depicts the road to the right of the car, and (d) to the left side.

- **Figure A.3b:** The usage of TR does not follow the RSSI samples trend as precisely, apart from the left side of the car. The closer it gets to the car, the less accurate the model prediction seems to be. This may have been caused due to the fact that the TR model considers grounds reflections which do not have as a bigger impact with obstructions as infrastructures do.

For this scenario we have plotted the error Histogram A.4. The error histograms where we compare to the free space counterpart were attached in the appendix of this document.

- **Histogram A.4a:** This histogram depicts that the usage of LD has about 47% of the results in a range of -5 dBm to 5 dBm difference to the samples, while using TR has about 43%. In the wider range of -10 dBm to 10 dBm, the usage of LD has about 77% of its values and TR about 75%. From these values, we believe we can affirm that LD has had better performance.
- **Histogram A.4b:** This histogram clearly demonstrates that the introduction of the attenuation caused by the bodies (L_B and L_C), from having 100% of the values overestimate to 47%

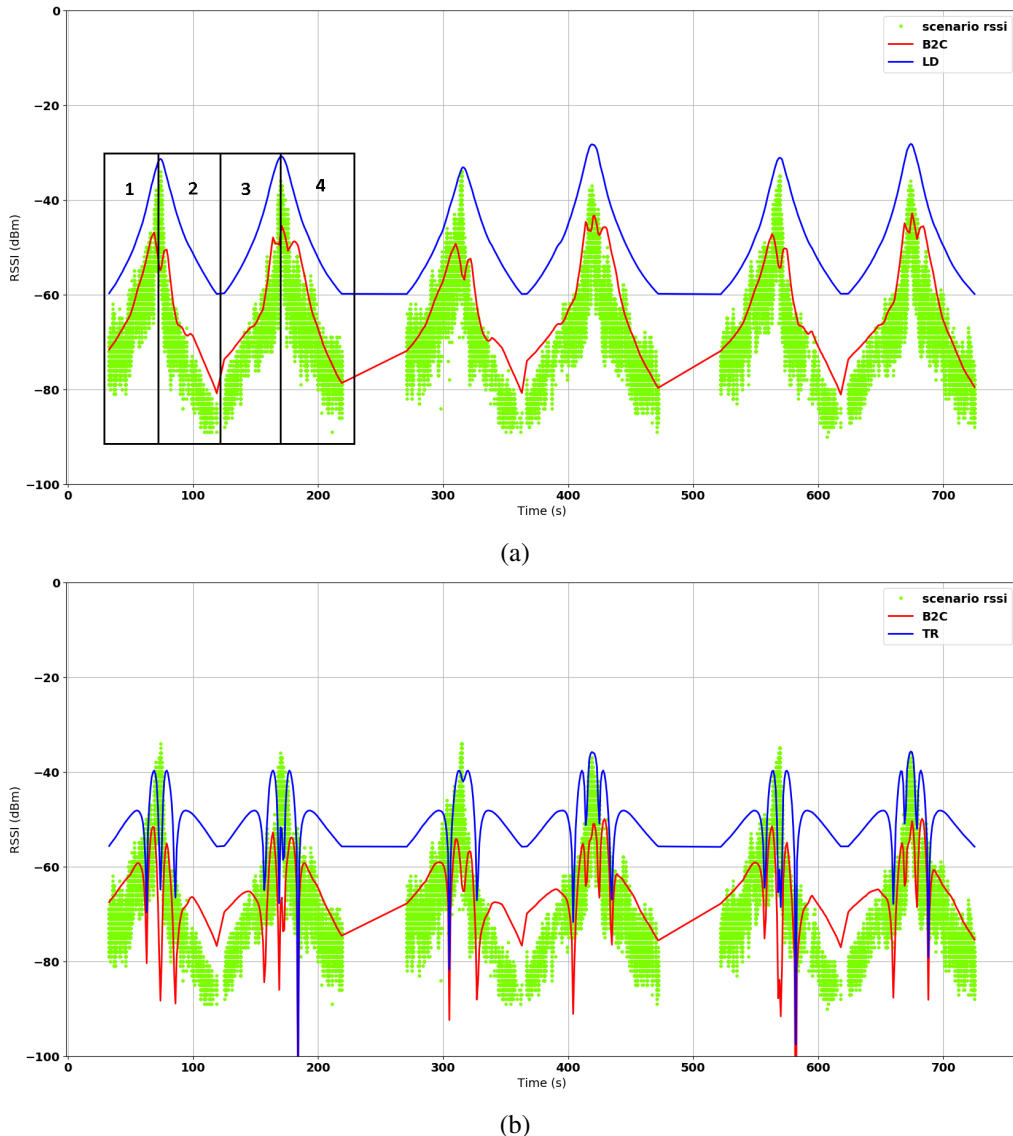


Figure A.3: RSSI Samples (green dots) from the **perpendicular scene without LoS**, overlaid with RSSI model prediction using either (a) Log Distance model or (b) Two-Rays model as the path loss component and comparison of the introduction of bicycle-cyclist and car's bodies (red line) to their absence (blue line).

in the ± 5 range. This does not make our model using LD reliable, but we do consider to have step in the right direction.

- **Histogram A.4c:** Just as LD, the usage of the TR component with L_B and L_C has also greatly improved. But, the distribution of values across the bins is caused by that big fluctuation of the model values, increasing the uncertainty of the proposed values.

Through this analyses we can confirm some expectations:

- The usage of LD than TR is more suited for scenarios that lack LoS.

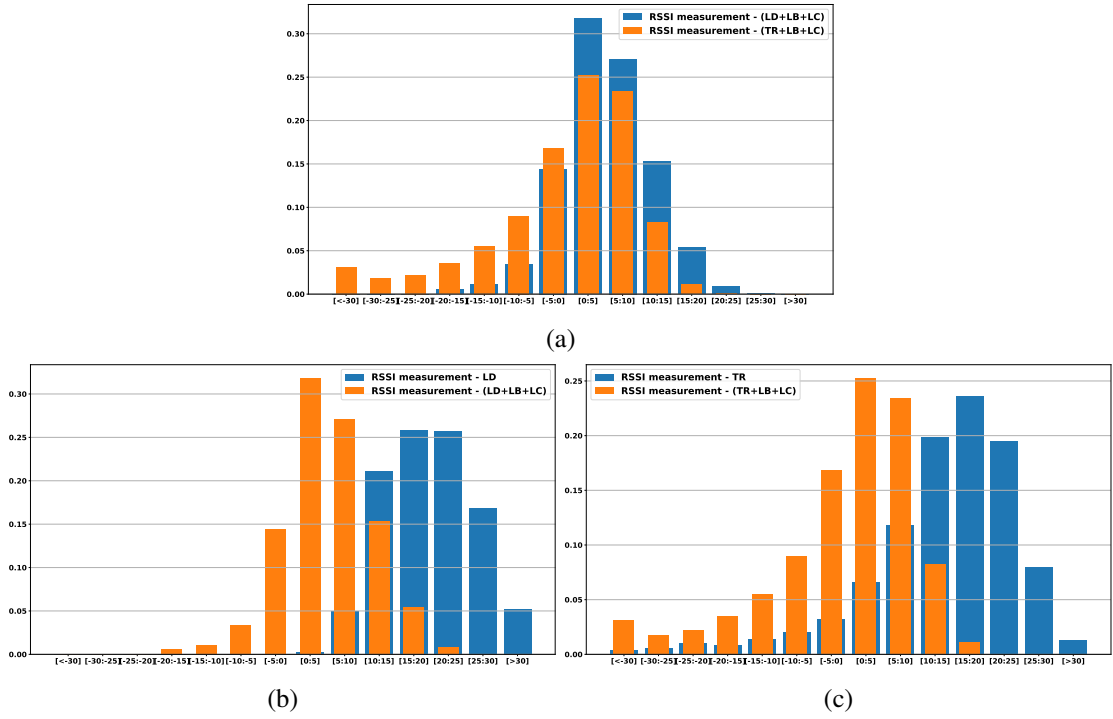


Figure A.4: Histograms of errors of the model for the perpendicular scene with LoS, using Log Distance, Two-Rays as path models, (a) comparing its performances between each other and their free space counterparts: (b) LD (c) TR

- The B2C model is less reliable for a link that include obstructions between a bicycle and a car (for TR in LoS, 63% of RSSI estimates fall within the [-5,5]dB error interval; in non-LoS, it is 43% of RSSI).

Bibliography

- [1] Flow. *15 quick facts for cities*. http://h2020-flow.eu/fileadmin/user_upload/Deliverables/15_quick_facts_eng_FINAL.pdf. Accessed: 2017-11-21. 2018.
- [2] NHTSA. *Bicyclists and other cyclists: 2015 data (Traffic Safety Facts. Report No. DOT HS 812 382)*. National Highway Traffic Safety Administration. Mar. 2017.
- [3] Statista. *Dossier on Cycling*. <https://www.statista.com/topics/1686/cycling/>. Accessed: 2017-11-21. 2017.
- [4] B. Kihei, J. A. Copeland, and Y. Chang. “Predicting Car Collisions Using RSSI”. In: *2015 IEEE Global Communications Conference (GLOBECOM)*. Dec. 2015, pp. 1–7. DOI: [10.1109/GLOCOM.2015.7417442](https://doi.org/10.1109/GLOCOM.2015.7417442).
- [5] Sandra Céspedes et al. “Poster: Smart networked bicycles with platoon cooperation”. In: *Vehicular Networking Conference (VNC), 2014 IEEE*. IEEE. 2014, pp. 199–200.
- [6] José Santa, Pedro J Fernández, and Miguel A Zamora. “Cooperative its for two-wheel vehicles to improve safety on roads”. In: *Vehicular Networking Conference (VNC), 2016 IEEE*. IEEE. 2016, pp. 1–4.
- [7] R. J. Weiler et al. “Environment Induced Shadowing of Urban Millimeter-Wave Access Links”. In: *IEEE Wireless Communications Letters* 5.4 (Aug. 2016), pp. 440–443. ISSN: 2162-2337. DOI: [10.1109/LWC.2016.2581820](https://doi.org/10.1109/LWC.2016.2581820).
- [8] S. Kaul et al. “Effect of Antenna Placement and Diversity on Vehicular Network Communications”. In: *2007 4th Annual IEEE Communications Society Conference on Sensor, Mesh and Ad Hoc Communications and Networks*. June 2007, pp. 112–121. DOI: [10.1109/SAHCN.2007.4292823](https://doi.org/10.1109/SAHCN.2007.4292823).
- [9] Theodore Rappaport. *Wireless Communications: Principles and Practice*. 2nd. Upper Saddle River, NJ, USA: Prentice Hall PTR, 2001. ISBN: 0130422320.
- [10] Kuang-Shih Huang et al. “Redeye: preventing collisions caused by red-light running scooters with smartphones”. In: *IEEE Transactions on Intelligent Transportation Systems* 17.5 (2016), pp. 1243–1257.

- [11] K. Dhondge et al. “WiFiHonk: Smartphone-Based Beacon Stuffed WiFi Car2X-Communication System for Vulnerable Road User Safety”. In: *2014 IEEE 79th Vehicular Technology Conference (VTC Spring)*. May 2014, pp. 1–5. DOI: [10.1109/VTCSpring.2014.7023146](https://doi.org/10.1109/VTCSpring.2014.7023146).
- [12] R. Parker and S. Valaee. “Vehicular Node Localization Using Received-Signal-Strength Indicator”. In: *IEEE Transactions on Vehicular Technology* 56.6 (Nov. 2007), pp. 3371–3380. ISSN: 0018-9545. DOI: [10.1109/TVT.2007.907687](https://doi.org/10.1109/TVT.2007.907687).
- [13] S. Hisaka and S. Kamijo. “On-board wireless sensor for collision avoidance: Vehicle and pedestrian detection at intersection”. In: *2011 14th International IEEE Conference on Intelligent Transportation Systems (ITSC)*. Oct. 2011, pp. 198–205. DOI: [10.1109/ITSC.2011.6082853](https://doi.org/10.1109/ITSC.2011.6082853).
- [14] Hao-Min Lin, Hsin-Mu Tsai, and Mate Boban. “Scooter-to-X communications: Antenna placement, human body shadowing, and channel modeling”. In: *Ad Hoc Networks* 37 (2016), pp. 87–100.
- [15] Richard Gass, James Scott, and Christophe Diot. “Measurements of in-motion 802.11 networking”. In: *Mobile Computing Systems and Applications, 2006. WMCSA’06. Proceedings. 7th IEEE Workshop on*. IEEE. 2005, pp. 69–74.
- [16] A. P. Subramanian et al. “Drive-By Localization of Roadside WiFi Networks”. In: *IEEE INFOCOM 2008 - The 27th Conference on Computer Communications*. Apr. 2008. DOI: [10.1109/INFOCOM.2008.122](https://doi.org/10.1109/INFOCOM.2008.122).
- [17] C. Sommer, S. Joerer, and F. Dressler. “On the applicability of Two-Ray path loss models for vehicular network simulation”. In: *2012 IEEE Vehicular Networking Conference (VNC)*. Nov. 2012, pp. 64–69. DOI: [10.1109/VNC.2012.6407446](https://doi.org/10.1109/VNC.2012.6407446).
- [18] Wantanee Viriyasitavat et al. “Vehicular Communications: Survey and Challenges of Channel and Propagation Models”. In: *Vehicular Technology Magazine, IEEE* 10 (May 2015), pp. 55–66. DOI: [10.1109/MVT.2015.2410341](https://doi.org/10.1109/MVT.2015.2410341).
- [19] Mate Boban, João Barros, and O.K. Tonguz. “Geometry-Based Vehicle-to-Vehicle Channel Modeling for Large-Scale Simulation”. In: *Vehicular Technology, IEEE Transactions on* 63 (May 2013). DOI: [10.1109/TVT.2014.2317803](https://doi.org/10.1109/TVT.2014.2317803).
- [20] D. Eckhoff, A. Brummer, and C. Sommer. “On the impact of antenna patterns on VANET simulation”. In: *2016 IEEE Vehicular Networking Conference (VNC)*. Dec. 2016, pp. 1–4. DOI: [10.1109/VNC.2016.7835925](https://doi.org/10.1109/VNC.2016.7835925).
- [21] TP-LINK. *TL-WN722N Datasheet*. Tech. rep. TP-LINK Technologies, 2010.
- [22] US Globalsat. *BU-353S4 GPS receiver*. Tech. rep. Globalsat Technology Corporation, 2009.
- [23] NLANR/DAST. *Iperf*. Software. <https://www.iperf.fr>. 2017.
- [24] Pedro Santos Pedro D Orey and Ana Aguiar José Pintor. “Opportunistic Use of In Vehicle Wireless Networks for Vulnerable Road User Interaction”. In: *IEEE Intelligent Vehicles Symposium* 1.1 (2018), pp. 1–2.

- [25] Filipe Neves et al. “Real-world Evaluation of IEEE 802.11P for Vehicular Networks”. In: *ACM International Workshop on Vehicular Inter-networking*. Las Vegas, Nevada, USA, 2011, pp. 89–90. ISBN: 978-1-4503-0869-4. DOI: [10.1145/2030698.2030717](https://doi.org/10.1145/2030698.2030717).